Published in final edited form as:
Biochemistry. 2012 October 16; 51(41): 8071–8084. doi:10.1021/bi3006658.

Spectroscopic and Functional Characterization of Iron-Sulfur Cluster-Bound Forms of *Azotobacter vinelandii* ^{Nif}IscA[†]

Daphne T. Mapolelo[⊥], **Bo Zhang**, **Sunil G. Naik**[§], **Boi Hanh Huynh**[§], and **Michael K. Johnson**[*]

[§]Department of Chemistry and Center for Metalloenzyme Studies, University of Georgia, Athens, Georgia, 30602, USA

[¶]Department of Physics, Emory University, Atlanta, Georgia 30322, USA

Abstract

The mechanism of [4Fe-4S] cluster assembly on A-type Fe-S cluster assembly proteins, in general, and the specific role of ^{Nif}IscA in the maturation of nitrogen fixation proteins are currently unknown. To address these questions, *in vitro* spectroscopic studies (UV–visible absorption/CD, resonance Raman and Mössbauer) have been used to investigate the mechanism of [4Fe-4S] cluster assembly on *Azotobacter vinelandii* ^{Nif}IscA, and the ability of ^{Nif}IscA to accept clusters from NifU and to donate clusters to the apo form of the nitrogenase Fe-protein. The results show that ^{Nif}IscA can rapidly and reversibly cycle between forms containing one $[2Fe\text{-}2S]^{2+}$ and one $[4Fe\text{-}4S]^{2+}$ cluster per homodimer via DTT-induced two-electron reductive coupling of two $[2Fe\text{-}2S]^{2+}$ clusters and O_2-induced $[4Fe\text{-}4S]^{2+}$ oxidative cleavage. This unique type of cluster interconversion in response to cellular redox status and oxygen levels is likely to be important for the specific role of A-type proteins in the maturation of [4Fe-4S] cluster-containing proteins under aerobic growth or oxidative stress conditions. Only the $[4Fe\text{-}4S]^{2+}$-^{Nif}IscA was competent for rapid activation of apo-nitrogenase Fe protein under anaerobic conditions. Apo-^{Nif}IscA was shown to accept clusters from [4Fe-4S] cluster-bound NifU via rapid intact cluster transfer, indicating a potential role as a cluster carrier for delivery of clusters assembled on NifU. Overall the results support the proposal that A-type proteins can function as carrier proteins for clusters assembled on U-type proteins and suggest that they are likely to supply [2Fe-2S] clusters rather than [4Fe-4S] for the maturation of [4Fe-4S] cluster-containing proteins under aerobic or oxidative stress growth conditions.

Iron sulfur (Fe-S) clusters are essential and versatile biological cofactors that are found in all organisms and are utilized in a wide range of physiologically processes, functioning not only in electron transport and as enzyme active sites, but also in DNA repair and sensing of ambient conditions for regulatory processes (1–4). Although Fe-S clusters are implicated in a wide range of biochemical processes, the detailed molecular mechanisms underlying their biosynthesis and repair remain to be elucidated. Ongoing studies on Fe-S cluster biosynthesis in eukaryotes and prokaryotes have led to the identification of highly conserved sets of genes which encode for proteins that are involved in the assembly of Fe-S clusters and their insertion into target apo-proteins (3,5–9). Besides the NIF system which is dedicated to maturation of the Fe-S proteins involved with nitrogen fixation in azototrophic bacteria, many bacteria contain the more general purpose ISC and SUF systems (5,7,8,10,11). In *E. coli*, the ISC system is utilized under normal growth conditions (12),

[†]This work was supported by grants from the NIH (GM62524 to M.K.J. and GM47295 to B.H.H.)

[*]To whom correspondence should be addressed: mkj@uga.edu; Tel: 706-542-9378; Fax: 706-542-9454.
[⊥]Current address: Department of Chemistry, University of Botswana, Botswana, Africa

while the SUF system is utilized under iron limitation and oxidative stress conditions (8,13–15). The bacterial ISC and SUF systems also constitute the major components of the Fe-S cluster biogenesis systems in mitochondria and chloroplasts, respectively (3,6,9).

A-type Fe-S cluster assembly proteins (^{Nif}IscA, IscA, SufA) are encoded by specific genes in the bacterial *nif*, *isc*, and *suf* operons, and constitute a homologous class of proteins with three rigorously conserved cysteine residues in a C-X_{63-65}-C-G-C sequence motif. In vitro studies have shown that the conserved cysteines are competent to ligate monomeric $Fe^{2+,3+}$ ions, $[2Fe\text{-}2S]^{2+}$ clusters or $[4Fe\text{-}4S]^{2+}$ clusters at the subunit interface of recombinant homodimers (16–18). However, the specific functions of A-type proteins in Fe-S cluster biogenesis have remained elusive, due in large part to the lack of a well-defined phenotype. Except for the A-type ErpA protein which has been shown to play a specific and essential role in the maturation of the key [4Fe-4S] cluster-containing enzymes (IspH and IspG) in the bacterial isoprenoid biosynthesis pathway (19), genetic studies indicate that A-type proteins often exhibit functional redundancy and are generally only required under aerobic or oxidative stress conditions. In *A. vinelandii*, which contains the NIF and SUF systems, deletion of ^{Nif}IscA (aka orf6) was found to have no effect on Mo-dependent diazotropic growth (20) and deletion of IscA was shown to be lethal only under elevated oxygen conditions (21). In *E. coli* knockouts of either IscA or SufA in *E. coli* have only mild effect on cell growth, while deletion of both IscA and SufA results in a null-growth phenotype in minimal medium under aerobic conditions (22,23). This has led to the discovery of specific roles for IscA/SufA in the maturation of bacterial $[4Fe\text{-}4S]^{2+}$ centers under aerobic growth conditions (24,25). A similar role has also been demonstrated in *S. cerevisiae*, where Isa1p and Isa2p have recently been shown to form an Fe-bound complex that is required, along the tetrahydrofolate-dependent Iba57 and Isu1p/Iscu2p, for the maturation of mitochondrial [4Fe-4S] proteins (26). However, a molecular level understanding of how A-type proteins facilitate [4Fe-4S] cluster maturation and whether this involves the mononuclear Fe or Fe-S cluster bound forms are still unresolved.

The objectives of this work and that of the accompanying manuscript were to address the role of mononuclear Fe- and Fe-S cluster-bound forms of *Azotobacter vinelandii* (*Av*) ^{Nif}IscA in NIF-specific Fe-S cluster biosynthesis using *in vitro* spectroscopic approaches. The simplicity of the NIF system, comprising NifS (cysteine desulfurase S-donor), NifU (primary scaffold protein) and ^{Nif}IscA, and its exclusive role in the maturation of nitrogen fixation proteins containing double or single [4Fe-4S] cubane clusters, make NIF an attractive system for investigating how A-type proteins facilitate [4Fe-4S] cluster maturation. The accompanying manuscript characterizes and addresses the role of mononuclear Fe-bound forms of *A. vinelandii* ^{Nif}IscA. This work focuses on characterizing and investigating the properties of Fe-S cluster-bound forms of *A. vinelandii* ^{Nif}IscA and addressing their role in [4Fe-4S] cluster maturation. The results demonstrate that ^{Nif}IscA can function as a carrier protein for clusters assembled on NifU and an effective cluster donor for maturation of the nitrogenase Fe protein under anaerobic conditions. Moreover the cluster-bound form of ^{Nif}IscA is shown to be reversibly dependent on medium conditions, with the dithiol reagent DTT favouring the $[4Fe\text{-}4S]^{2+}$ cluster-bound homodimer under anaerobic conditions and O_2 exposure resulting in conversion to the $[2Fe\text{-}2S]^{2+}$ cluster-bound homodimer. The mechanism of the cluster interconversion and the potential importance of both the $[4Fe\text{-}4S]^{2+}$ and $[2Fe\text{-}2S]^{2+}$ cluster-bound forms of A-type proteins for the maturation [4Fe-4S] cluster-containing proteins under anaerobic, aerobic or oxidative stress conditions are discussed in light of these results.

MATERIALS AND METHODS

Materials

Materials used in this work were of reagent grade and were purchased from Fischer Scientific, Sigma-Aldrich Chemical Co, Invitrogen, VWR International, unless otherwise stated.

Expression and Purification of Av ^{Nif}IscA

The procedures used for the heterologous expression and purification of *A. vinelandii* ^{Nif}IscA are described in the accompanying manuscript. All samples used in this work were > 95% pure based on gel electrophoresis and direct amino acid analyses conducted at Texas A&M University.

Biochemical Analyses

Protein and iron assays of Fe-S cluster-bound forms of *Av* ^{Nif}IscA were carried our as described in the accompanying manuscript. Protein concentrations of *Av* ^{Nif}IscA were assessed using the BioRad Dc protein assay and corrected for a 17% overestimate based on direct amino acid analysis (see preceding paper). The oligomeric state of $[2Fe\text{-}2S]^{2+}$ cluster-bound ^{Nif}IscA was determined by analytical gel-filtration chromatography using a 25 mL Superdex G-75 10/300 column (Pharmacia Biotech), as described in the accompanying manuscript.

Spectroscopic Methods

Samples for all spectroscopic investigations were prepared under argon atmosphere in a glove box (Vacuum Atmosphere, Hawthorne, CA) at oxygen levels < 1 ppm. UV–visible absorption spectra were recorded under anaerobic conditions in septum-sealed 1 mm quartz cuvettes or small-volume 1 cm cuvettes at room temperature, using a Shimadzu UV-3101 PC scanning spectrophotometer fitted with a TCC-260 temperature controller. CD spectra were also recorded under anaerobic conditions in the same cuvettes using a JASCO J-715 spectropolarimeter (Jasco, Easton, MD). Resonance Raman spectra were recorded at 17 K as previously described (27), using a Ramanor U1000 spectrometer (Instruments SA, Edison, NJ) coupled with a Sabre argon ion laser (Coherent, Santa Clara, CA), with 20 μL frozen droplets of sample mounted on the cold finger of a Displex Model CSA-202E closed cycle refrigerator (Air Products, Allentown, PA). X-band (~ 9.6 GHz) EPR spectra were recorded using a ESP-300E spectrometer (Bruker, Billerica, MA), equipped with an ER-4116 dual mode cavity and an ESR-900 helium flow cryostat (Oxford Instruments, Concord, MA). Mössbauer spectra in the presence of applied magnetic fields were recorded using previously described instrumentation (28), and the data was analyzed with the WMOSS program (Web Research).

NifS-mediated Fe-S Cluster Assembly on ^{Nif}IscA

Cluster-bound ^{Nif}IscA was prepared by first pre-treating as-purified apo ^{Nif}IscA in 100 mM Tris-HCl buffer at pH 7.8 (buffer A) with 20-fold excess of tris(2-carboxyethyl)phosphine hydrochloride (TCEP) for 30 min in order to cleave disulfides/polysulfides. The protein was then exchanged into buffer A containing 150 mM NaCl using a 50 mL G-25 desalting column (GE Healthcare) previously equilibrated with the same buffer. The eluted protein was concentrated using a YM10 Amicon. TCEP-treated ^{Nif}IscA (1 mM) was incubated with NifS (6.27 μM), ferrous ammonium sulfate (4 mM) and L-cysteine (16 mM) in the same buffer for 45 min in an ice bath under anaerobic conditions in a Vacuum Atmospheres glove box under argon (<1 ppm O_2). Protein concentrations of ^{Nif}IscA and NifS are reported as monomers. For Mössbauer samples, ^{57}Fe-enriched ferrous ammonium sulfate (>95%

enrichment) was used in the reconstitution mixture in place of natural abundance ferrous sulfate. Mössbauer studies of the time course of Fe-S cluster assembly on ^{Nif}IscA were carried out by taking out aliquots of the reaction mixture at different time intervals, placing in Mössbauer cups and freezing in liquid nitrogen. For Mössbauer control experiments, samples were prepared as above except that ^{Nif}IscA was omitted from the reaction mixture. UV–visible absorption and CD studies of the time course of Fe-S cluster assembly were carried at different time intervals on one sample under anaerobic conditions in septum-sealed 1 mm quartz cuvettes at room temperature. Purification of cluster-bound ^{Nif}IscA to remove excess reagents was achieved by loading the reconstitution mixture onto 2×5 mL High-trap Q-Sepharose column (GE Healthcare) previously equilibrated with buffer A and eluted with a 0–100 % NaCl gradient from buffer A containing 1 M NaCl. The $[2Fe\text{-}2S]^{2+}$ cluster-bound form of ^{Nif}IscA eluted between 0.45 and 0.55 M NaCl and was concentrated using a YM10 Amicon. Incubation of $[2Fe\text{-}2S]^{2+}$ cluster-bound ^{Nif}IscA with 2 mM DTT under anaerobic conditions in buffer A for 15 min yielded the $[4Fe\text{-}4S]^{2+}$ cluster-bound form of ^{Nif}IscA.

Holo ^{Nif}IscA to Apo ADP-bound Nitrogenase Fe Protein Cluster Transfer

The apo form of ADP-bound *A. vinelandii* nitrogenase Fe protein was prepared as previously described (29). Reactions were carried out in buffer A and $[2Fe\text{-}2S]^{2+}$ cluster-bound ^{Nif}IscA was incubated with 2 mM DTT in the same buffer for 15 min prior to use in cluster transfer experiments. The time course of cluster transfer from 2 mM DTT treated $[2Fe\text{-}2S]^{2+}$ cluster-bound ^{Nif}IscA to apo ADP-bound nitrogenase Fe protein was monitored under anaerobic conditions in small-volume 1 cm cuvettes at room temperature using UV–visible absorption and CD spectroscopies. After 50 min, the cluster transfer mixture was loaded onto a 2×5 mL High-trap Q-Sepharose column (GE Healthcare) pre-equilibrated with buffer A. The columns were then washed with 3 bed volumes of the same buffer. Both proteins eluted with a 0 – 100 % NaCl gradient from buffer A containing 1 M NaCl with apo ^{Nif}IscA and holo Fe protein eluting between 0.45–0.55 and 0.65–0.70 M NaCl respectively. The greenish-brown fractions of the Fe protein were concentrated using a YM30 Amicon and used for EPR studies after anaerobic addition of 50% (v/v) ethylene glycol and reduction with sodium dithionite and rapid freezing in liquid nitrogen.

Holo NifU to apo ^{Nif}IscA cluster transfer

Reactions were carried out in buffer A and [4Fe-4S] cluster-bound NifU was prepared as described previously (30). The time course of cluster transfer from $[4Fe\text{-}4S]^{2+}$ cluster-bound NifU to TCEP-pretreated apo-^{Nif}IscA in the absence and presence of DTT was monitored under anaerobic conditions in septum-sealed small-volume 1 cm cuvettes at room temperature using UV–visible absorption and CD spectroscopy.

RESULTS

NifS-mediated Fe-S cluster assembly on ^{Nif}IscA

UV-visible absorption/CD and Mössbauer spectroscopies were used to characterize the time course of NifS-catalyzed cluster assembly on ^{Nif}IscA. The UV–visible absorption and CD spectra of apo ^{Nif}IscA and of the reconstitution mixture taken after 5 min, 20 min, and 65 min of NifS-mediated cluster reconstitution are shown in Figure 1. No significant visible absorption or CD that can be attributed to S-to-Fe(III) charge-transfer transitions of an Fe-S cluster is observed after 5 min. However, after 20 min, the characteristic visible absorption and CD spectrum of ^{Nif}IscA containing one $[2Fe\text{-}2S]^{2+}$ cluster per homodimer is observed (see below). Based on the CD $\Delta\varepsilon$ values per $[2Fe\text{-}2S]^{2+}$ cluster that were determined for dimeric ^{Nif}IscA samples of known $[2Fe\text{-}2S]^{2+}$ cluster content as determined by analytical and Mössbauer (see below), it is estimated that the reconstitution mixture contains 30–40%

of the ^{Nif}IscA in a form containing one $[2Fe\text{-}2S]^{2+}$ cluster per homodimer. As the reaction proceeds, the UV–visible absorption intensity increases and after 65 min is dominated by a broad shoulder centered at 420 nm which is more characteristic of a $[4Fe\text{-}4S]^{2+}$ cluster (31). Concomitantly, the UV–visible CD of the $[2Fe\text{-}2S]^{2+}$ center decreases and is almost completely lost after 65 min. As shown below, $[4Fe\text{-}4S]^{2+}$ centers on ^{Nif}IscA exhibit negligible CD intensity compare to $[2Fe\text{-}2S]^{2+}$ centers. Consequently, the UV-visible CD and absorption data are consistent with $[2Fe\text{-}2S]^{2+}$ to $[4Fe\text{-}4S]^{2+}$ cluster conversion, but this clearly requires confirmation using Mössbauer spectroscopy which provides positive identification and quantitation of both $[2Fe\text{-}2S]^{2+}$ and $[4Fe\text{-}4S]^{2+}$ clusters in a reaction mixture.

Mössbauer spectroscopy was used in a previous study to characterize the time course of steady state NifS-mediated cluster assembly on ^{Nif}IscA (17). The same approach was used in this study to complement the UV-visible absorption and CD results discussed above. The major differences were that the samples of apo ^{Nif}IscA used in this work were pre-treated with TCEP rather than DTT to cleave disulfides and were taken from the reaction at different time intervals and frozen for Mössbauer studies, rather than being subjected to cycles of thawing and freezing to generate Mössbauer samples at different time intervals. Figure 2, left panel, shows Mössbauer spectra (dotted lines) of samples taken from NifS-mediated reconstitution of ^{Nif}IscA reaction mixture at 2 min (A), 20 min (B), and 60 min (C). The Mössbauer spectra of control samples taken from an identical reaction mixture that lacked ^{Nif}IscA at the same time intervals are shown in the right panel of Figure 2. The colored lines are theoretical simulations for the individual Fe species using the Mössbauer parameters listed in Table 1, with the three high-spin Fe(II) components, termed $Fe^{II}Cys_4$, Fe^{II}-3.5 and Fe^{II}-4.1, shown in green and $[2Fe\text{-}2S]^{2+}$ clusters and $[4Fe\text{-}4S]^{2+}$ clusters shown in red and blue, respectively. They are plotted in accord with the percentage absorptions listed in Table 2. The solid black lines overlaid with the experimental spectra are the composites of these simulated spectra. The labelling of the three high-spin ferrous ions is adapted from Krebs *et al* (17) where $Fe^{II}Cys_4$, is tetrahedral sulfur coordinated Fe^{2+} ion and Fe^{II}-3.5 and Fe^{II}-4.1 are labelled according to their quadrupole splitting parameters (ΔE_Q), ΔE_{Q1}= 3.5 mm/s and ΔE_{Q2}= 4.1 mm/s respectively.

Analysis of the Mössbauer data shows that after 2 min of the ^{Nif}IscA reconstitution reaction, an overwhelming majority (98%) of the Fe is present as high-spin ferrous species while a small minority (~2%) is present as $[4Fe\text{-}4S]^{2+}$ cluster (Figure 2A and Table 2). However similar data, with ~2% of the Fe present as $[4Fe\text{-}4S]^{2+}$ cluster, were observed in the control experiment without ^{Nif}IscA (Figure 2D and Table 2), indicating that the $[4Fe\text{-}4S]^{2+}$ clusters are bound by exogenous cysteine rather than ^{Nif}IscA. As the reaction progresses to 20 min, the ^{Nif}IscA reconstitution sample shows formation of $[2Fe\text{-}2S]^{2+}$ and $[4Fe\text{-}4S]^{2+}$ clusters with percentage iron absorptions of 9% and 11% respectively, with the rest of the Fe attributed to high-spin ferrous species (Figure 2B and Table 2). Based on the ^{57}Fe ferrous ammonium sulfate concentration of 4 mM and the monomeric ^{Nif}IscA concentration of 1 mM, this translates to $[2Fe\text{-}2S]^{2+}$ and $[4Fe\text{-}4S]^{2+}$ cluster concentrations of 0.18 mM and 0.11 mM, respectively, or 36% of the ^{Nif}IscA present in a form containing one $[2Fe\text{-}2S]^{2+}$ per homodimer and 22% of the ^{Nif}IscA present in a form containing one $[4Fe\text{-}4S]^{2+}$ per homodimer. The control sample indicates that $[4Fe\text{-}4S]^{2+}$ concentration is likely to be an overestimate, as 5% of the Fe in the reaction mixture without ^{Nif}IscA was found to be present as exogenous cysteine-ligated $[4Fe\text{-}4S]^{2+}$ clusters (Figure 2E and Table 2), which translates to a $[4Fe\text{-}4S]^{2+}$ cluster concentration of 0.05 mM. With a longer reaction time of 60 min, the accumulation of $[4Fe\text{-}4S]^{2+}$ clusters increases to 41% of the total Fe (Figure 2C and Table 2) which corresponds to a $[4Fe\text{-}4S]^{2+}$ cluster concentration of 0.41 mM or 82% of the ^{Nif}IscA present in a form containing one $[4Fe\text{-}4S]^{2+}$ per homodimer, along with concomitant decrease in the $[2Fe\text{-}2S]^{2+}$ cluster contribution to 3% of the total Fe (0.06 mM

in $[2Fe\text{-}2S]^{2+}$ clusters or 12% of the ^{Nif}IscA present in a form containing one $[2Fe\text{-}2S]^{2+}$ per homodimer). The concentration of $[4Fe\text{-}4S]^{2+}$ clusters in the control sample without ^{Nif}IscA remains approximately constant at 6% of the total Fe or 0.06 mM in exogenous cysteine-ligated $[4Fe\text{-}4S]^{2+}$ clusters (Figure 2F and Table 2). Hence, ~70% of the ^{Nif}IscA present in a form containing one $[4Fe\text{-}4S]^{2+}$ per homodimer. In agreement with previous results (17), the Mössbauer and UV–visible absorption and CD results presented herein suggest that a form of ^{Nif}IscA containing one $[4Fe\text{-}4S]^{2+}$ cluster per homodimer is assembled via a species containing one $[2Fe\text{-}2S]^{2+}$ cluster per homodimer under steady state conditions of NifS-mediated cluster assembly. The only major difference between the two sets of results is slower rates of $[2Fe\text{-}2S]^{2+}$ cluster assembly in the present study which is attributed to lower PLP content and hence activity for the NifS samples used in this work. The present work also demonstrates that CD can be effectively used as a convenient, selective and quantitative monitor of the $[2Fe\text{-}2S]^{2+}$ cluster-bound form of ^{Nif}IscA.

The mechanism of NifS-mediated $[4Fe\text{-}4S]^{2+}$ cluster assembly on ^{Nif}IscA via a $[2Fe\text{-}2S]^{2+}$ intermediate under reconstitution conditions has yet to be determined. However the ability of DTT to effect $[2Fe\text{-}2S]^{2+}$ to $[4Fe\text{-}4S]^{2+}$ cluster conversion on ^{Nif}IscA in the absence of O_2 suggests two-electron reductive coupling of two $[2Fe\text{-}2S]^{2+}$ at the subunit interface of a homodimer (see below). This raises the question of the source of reducing equivalents during NifS-mediated reconstitution in the absence of DTT. The most likely candidate is disulfide formation by the cysteines that are released during reductive coupling.

Purification and characterization of $[2Fe\text{-}2S]^{2+}$ cluster-bound ^{Nif}IscA

In accord with the results of Krebs et al (17), attempts to purify homogeneous samples of the $[4Fe\text{-}4S]^{2+}$ cluster-bound form of ^{Nif}IscA from the NifS-mediated reconstitution mixture after 65 min of reaction were unsuccessful. Despite numerous attempts using anaerobic conditions (<1 ppm O_2 inside the glove box) and low temperatures (10 °C), the $[4Fe\text{-}4S]^{2+}$ cluster-bound form of the ^{Nif}IscA was found to revert back partially or completely to the $[2Fe\text{-}2S]^{2+}$ cluster-bound form during purification using a Q-sepharose column in the absence of DTT. Based on the resulted discussed below, this is most likely a consequence of traces of O_2 in the buffer solutions that were degassed outside the glove box and used to wash and elute ^{Nif}IscA from the column. However, many of the resultant $[2Fe\text{-}2S]^{2+}$ cluster-bound forms of ^{Nif}IscA, were more homogeneous than previously characterized samples (17) and hence more conducive to detailed analytical and spectroscopic characterization. The UV–visible absorption and CD spectra of anaerobically purified ^{Nif}IscA are shown in Figure 3. The UV–visible spectrum of cluster-bound ^{Nif}IscA is dominated in the 300-to-600-nm region by bands centered at 331 nm and 425 nm with the latter having a shoulder at 463 nm and an unresolved broad band centered at 555 nm. These absorption bands correlate with UV–visible CD bands: positive bands centered at 348, 456, 522, and 630 nm and negative bands centered at 318, 395 and 566 nm. Both the UV–visible absorption and CD spectra are characteristic of a $[2Fe\text{-}2S]^{2+}$ cluster (32;33). Quantitative gel filtration chromatography revealed a molecular mass of ~25 kDa for apo- and [2Fe-2S]-^{Nif}IscA. Since the predicted molecular mass of Av^{Nif}IscA is 11,047 Da, this suggests that both the apo- and $[2Fe\text{-}2S]^{2+}$ cluster-bound forms of ^{Nif}IscA are present as a dimers in solution. Fe and protein analytical data from six different preparations indicated that the reconstituted samples contained 0.79 ± 0.10 Fe per ^{Nif}IscA monomer. Since Mössbauer data for these samples reveal that all the Fe in these sample is present as $[2Fe\text{-}2S]^{2+}$ clusters (see below), the Fe and protein analytical data correspond to 0.79 ± 0.10 $[2Fe\text{-}2S]^{2+}$ clusters per homodimeric ^{Nif}IscA. Although we have yet been able to prepare samples with 1.0 $[2Fe\text{-}2S]^{2+}$ clusters per homodimeric ^{Nif}IscA, taken together with the crystallographic data for *T. elongatus* IscA (18), the analytical data clearly supports a maximal stoichiometry of one $[2Fe\text{-}2S]^{2+}$ cluster per homodimeric ^{Nif}IscA. Since the UV–visible absorption spectra of these samples indicate

a molar extinction coefficient at 425 nm (ε_{425}) of 4.03 ± 0.20 mM^{-1} cm^{-1} based on ^{Nif}IscA monomer, see Figure 3, the analytical data indicate ε_{425} = 10.0 ± 1.0 mM^{-1} cm^{-1} per $[2Fe\text{-}2S]^{2+}$ cluster. This molar extinction coefficient was used to quantify the $[2Fe\text{-}2S]^{2+}$ cluster content of all purified $[2Fe\text{-}2S]^{2+}$ cluster-bound samples of ^{Nif}IscA used in this work.

The vibrational properties of the Fe-S cluster in ^{Nif}IscA were characterized by resonance Raman spectroscopy. The resonance Raman spectra of $[2Fe\text{-}2S]^{2+}$ cluster-bound ^{Nif}IscA in the Fe–S stretching region (240 – 450 cm^{-1}), obtained using 457.9, 487.9 and 514.5-nm excitation, comprises an intense band at 290 cm^{-1} and additional bands at 338, 358, 396, and 421 cm^{-1}, see Figure 4. The spectra are similar to those reported previously for the $[2Fe\text{-}2S]^{2+}$ cluster-bound form of ^{Nif}IscA using 457.9-nm excitation (17), albeit with greatly improved signal-to-noise ratio and the observation of additional weak bands. The spectra are relatively insensitive to excitation wavelength and the improved quality data enable vibrational assignments to be made by direct comparison with vibrationally well-characterized $[2Fe\text{-}2S]^{2+}$ centers in simple ferredoxins such as *S. oleracea* ferredoxin, bovine adrenodoxin, and *P. putida* putidaredoxin (34), see Table 3. The Fe-S stretching frequencies for the $[2Fe\text{-}2S]^{2+}$ center in ^{Nif}IscA are very similar to those of the all-cysteine ligated $[2Fe\text{-}2S]^{2+}$ centers in simple ferredoxins, strongly suggesting analogous cluster ligation in ^{Nif}IscA. Further evidence for an all-cysteinyl-ligated $[2Fe\text{-}2S]^{2+}$ cluster in re-purified reconstituted ^{Nif}IscA and definitive assessment of the cluster composition were provided by Mössbauer spectroscopy, see Figure 5A. The Mössbauer spectrum is well fit by the quadrupole doublet characteristic of an $S = 0$ $[2Fe\text{-}2S]^{2+}$ cluster, composed of two antiferromagnetically coupled high-spin Fe^{3+} sites (δ = 0.28 mm/s and ΔE_Q = 0.68 mm/s for site 1 and δ = 0.27 mm/s and ΔE_Q = 0.50 mm/s for site 2). The similarity and value of the isomer shift parameter (δ) for each Fe site of the $[2Fe\text{-}2S]^{2+}$ cluster are consistent with tetrahedral S ligation at each Fe site. Hence, in accord with the crystallographic data for $[2Fe\text{-}2S]^{2+}$ cluster-bound *T. elongatus* IscA (18), the Mössbauer and resonance Raman results provide compelling evidence for complete cysteinyl ligation for the $[2Fe\text{-}2S]^{2+}$ clusters on ^{Nif}IscA in solution.

DTT-induced $[2Fe\text{-}2S]^{2+}$ to $[4Fe\text{-}4S]^{2+}$ cluster conversion on ^{Nif}IscA

In vitro studies of SufA have reported that the $[2Fe\text{-}2S]^{2+}$ cluster-bound form is competent for maturation of [4Fe-4S] cluster-containing proteins in the presence of DTT (35). In order to understand how the $[2Fe\text{-}2S]^{2+}$ cluster-bound form of an A-type protein can effect maturation of [4Fe-4S] cluster-containing proteins and rationalize *in vivo* data which indicate a specific role for A-type proteins in the maturation of [4Fe-4S] cluster-containing proteins in mitochondria (26,36–38) and in bacteria under aerobic growth conditions (24), we have investigated the mechanism of [4Fe-4S] cluster assembly on *A. vinelandii* ^{Nif}IscA. The UV–visible absorption and CD spectra of $[2Fe\text{-}2S]^{2+}$ cluster-bound ^{Nif}IscA (0.05 mM in $[2Fe\text{-}2S]^{2+}$ clusters) before (solid red line) and 15 min after addition of 2 mM DTT under strictly anaerobic conditions (solid blue line) are shown in Figure 6. On addition of DTT, the visible absorption spectrum of the $[2Fe\text{-}2S]^{2+}$ cluster is bleached over a period of approximately 15 min to yield an absorption spectrum with a pronounced shoulder at ~400 nm that is characteristic of a $[4Fe\text{-}4S]^{2+}$ cluster. Parallel CD studies indicate that 15 min after the addition of DTT, the amount of $[2Fe\text{-}2S]^{2+}$ cluster-bound ^{Nif}IscA has decreased to ~16% of the original level and imply that any new cluster-bound forms generated have negligible CD, which is consistent with the formation of a $[4Fe\text{-}4S]^{2+}$ cluster as demonstrated by the Mössbauer-monitored NifS-mediated reconstitution results discussed above.

More direct evidence for DTT-induced $[2Fe\text{-}2S]^{2+}$ to $[4Fe\text{-}4S]^{2+}$ cluster conversion on ^{Nif}IscA and quantitation of the cluster conversion process were provided by parallel Mössbauer studies, see Figure 5A–C and Tables 1 and 4. The distinct isomer shift (δ) and

quadrupole splitting (ΔE_Q) parameters of the ^{Nif}IscA-bound $[2Fe\text{-}2S]^{2+}$ and $[4Fe\text{-}4S]^{2+}$ clusters enable Mössbauer spectroscopy to quantitatively monitor the cluster conversion. Mössbauer spectra of $[2Fe\text{-}2S]^{2+}$ cluster-bound ^{Nif}IscA (0.5 mM in $[2Fe\text{-}2S]^{2+}$ clusters) were recorded before (A) and after incubation with 2 mM DTT for 1 min (B) and 15 min (C). The solid lines overlaid with the experimental spectra (hashed marks) are the composite simulations based on overlapping spectra from $[2Fe\text{-}2S]^{2+}$ clusters (red), $[4Fe\text{-}4S]^{2+}$ clusters (blue) and a mononuclear high-spin Fe(II) species (green), using the Mössbauer parameters listed in Table 1 and percentage Fe contributions listed in Table 4. Prior to addition of DTT, all the Fe in reconstituted and re-purified ^{Nif}IscA is in the form of $[2Fe\text{-}2S]^{2+}$ clusters. However, the cluster composition changes dramatically on addition of 2 mM DTT. After 1 min, 43% of the Fe has been converted to $[4Fe\text{-}4S]^{2+}$ clusters and 10% to a mononuclear ferrous species, with 34% remaining as $[2Fe\text{-}2S]^{2+}$ clusters. After 15 min, 53% of the Fe has been converted to $[4Fe\text{-}4S]^{2+}$ clusters and 18% to a mononuclear ferrous species, with only 16% remaining as $[2Fe\text{-}2S]^{2+}$ clusters. The extent to which the $[2Fe\text{-}2S]^{2+}$ clusters are lost as a function of time closely parallels the CD data discussed above. The mononuclear Fe(II) species in both the 1 min and 15 min samples has Mössbauer parameters very similar to those of Fe(II)-bound ^{Nif}IscA, see accompanying manuscript. The remaining Fe in both samples (~13%) is primarily present as a paramagnetic species with absorption spanning a range from 3.0 to +3.5 mm/s that is attributed to $S = 1/2$ $[2Fe\text{-}2S]^{+}$ clusters, based on similarity to Mössbauer spectra of reduced $[2Fe\text{-}2S]^{+}$ clusters in ferrochelatase (39) and ferredoxins (40) and parallel EPR data, see below. While the appearance of a mononuclear ferrous species indicates that the cluster conversion proceeds with up to 20% degradation of the initial $[2Fe\text{-}2S]^{2+}$ clusters, it is clear that the majority of the $[2Fe\text{-}2S]^{2+}$ clusters have been converted into $[4Fe\text{-}4S]^{2+}$ clusters on incubation with DTT.

EPR spectroscopy was used to identify the paramagnetic species that contributes to the Mössbauer spectrum in the presence of DTT and thereby assess the mechanism of the cluster formation process. While $[2Fe\text{-}2S]^{2+}$ cluster-bound form of ^{Nif}IscA showed no EPR signals, samples frozen within 5 s of DTT addition showed a broad rhombic $S = 1/2$ resonance with $g = 2.01$, 1.97 and 1.92 that accounted for 0.15 spins/[2Fe-2S] cluster, see Figure 7. The signal persisted, albeit with reduced intensity corresponding to 0.10 spins/[2Fe-2S] cluster, for samples frozen 15 min after addition of DTT. The signal is assigned to a $S = 1/2$ $[2Fe\text{-}2S]^{+}$ cluster rather than a $S = 1/2$ $[4Fe\text{-}4S]^{+}$ cluster based on relaxation properties. The resonance readily undergoes power saturation at 4.2 K and is observable without significant broadening at 70 K. This indicates slow relaxation which is typical of $S = 1/2$ $[2Fe\text{-}2S]^{+}$ clusters, whereas $S = 1/2$ $[4Fe\text{-}4S]^{+}$ cluster are much faster relaxing and broaden significantly above 30 K. On the basis that (1) the paramagnetic species exhibits Mössbauer spectra with major features similar to those detected for $S = 1/2$ $[2Fe\text{-}2S]^{+}$ centers, (2) EPR data show a paramagnetic species attributable to a $S = 1/2$ $[2Fe\text{-}2S]^{+}$ cluster, and (3) the paramagnetic Mössbauer and EPR species both account for 10–15 % of the initial [2Fe-2S] cluster concentration, we assign both to one-electron reduced $S = 1/2$ $[2Fe\text{-}2S]^{+}$ clusters. The observation of a $[2Fe\text{-}2S]^{+}$ cluster intermediate in the formation of $[4Fe\text{-}4S]^{2+}$ clusters on ^{Nif}IscA implies that the $[4Fe\text{-}4S]^{2+}$ clusters are formed by reductive coupling of two $[2Fe\text{-}2S]^{2+}$ clusters at the subunit interface.

Based on CD studies, no $[2Fe\text{-}2S]^{2+}$-to-$[4Fe\text{-}4S]^{2+}$ cluster conversion was observed on addition of 3 mM cysteine or glutathione (GSH) to $[2Fe\text{-}2S]^{2+}$-^{Nif}IscA under anaerobic conditions. Hence it would appear that the lower redox potential of the dithiol/disulfide couple in DTT (−340 mV at pH 7.4), compare to cysteine/cystine (−250 mV at pH 7.4) or GSH/GSSG (−260 mV at pH 7.4) (41), is required for reductive coupling to form $[4Fe\text{-}4S]^{2+}$ clusters on ^{Nif}IscA.

O_2-induced $[4Fe\text{-}4S]^{2+}$ to $[2Fe\text{-}2S]^{2+}$ cluster conversion on ^{Nif}IscA

Since A-type proteins have been implicated in having a role in the maturation of bacterial [4Fe-4S] cluster-containing proteins under aerobic growth conditions, Mössbauer and UV-visible absorption and CD spectroscopies were also used to assess the effect of O_2 exposure on the $[4Fe\text{-}4S]^{2+}$ clusters generated by incubation of $[2Fe\text{-}2S]^{2+}$ cluster-bound ^{Nif}IscA with DTT. Hence the Mössbauer sample containing 53% of the Fe as $[4Fe\text{-}4S]^{2+}$ clusters, that was generated by treating $[2Fe\text{-}2S]^{2+}$ cluster-bound ^{Nif}IscA with 2 mM DTT for 15 min, was thawed and exposed to air for 5 min before refreezing for Mössbauer analysis, see Figure 5D. The Mössbauer data clearly demonstrate that O_2 reverses the DTT-induced $[4Fe\text{-}4S]^{2+}$ to $[2Fe\text{-}2S]^{2+}$ cluster conversion, as the resulting sample has 60% of the Fe in $[2Fe\text{-}2S]^{2+}$ clusters and 15% in $[4Fe\text{-}4S]^{2+}$ clusters, with the remaining 25% as unresolved broad ferric species, see Table 5. In comparison with the 18% of mononuclear Fe(II) species detected in the DTT-treated starting sample, the observed 25% ferric species represents a minor loss of Fe during O_2 exposure. On the basis of the intensity of the characteristic $g = 5.5$ resonance that was observed in parallel EPR samples, compared to samples of Fe(III)-bound ^{Nif}IscA of known concentration (see accompanying manuscript), approximately 80% of the ferric species is present as $S = 3/2$ Fe(III)-bound ^{Nif}IscA. Hence the majority of Fe released remains ^{Nif}IscA-bound in the O_2-exposed samples.

UV–visible absorption and CD spectroscopy provides a convenient method for monitoring ^{Nif}IscA $[4Fe\text{-}4S]^{2+} \leftrightarrow [2Fe\text{-}2S]^{2+}$ cluster interconversions in real time without repeated freeze-thaw cycles. Hence this approach was used to investigate the reversibility of this cluster transformation, see Figure 6. As previously demonstrated, the predominantly $[4Fe\text{-}4S]^{2+}$ cluster-containing form of ^{Nif}IscA (blue line) was initially generated by incubating the as-purified $[2Fe\text{-}2S]^{2+}$ cluster-containing form (red line) with DTT for 15 min under anaerobic conditions. The $[4Fe\text{-}4S]^{2+}$ cluster-bound form of homodimeric ^{Nif}IscA was then exposed to O_2 by uncapping the cuvette in air at room temperature for 5 min before recapping and immediately recording spectra. The UV–visible absorption and CD spectra indicate that $[4Fe\text{-}4S]^{2+}$ cluster undergoes oxidative cleavage to yield the original $[2Fe\text{-}2S]^{2+}$ cluster-bound form of homodimeric ^{Nif}IscA (broken red line) in ~75% yield based on the initial $[2Fe\text{-}2S]^{2+}$ cluster CD intensity prior to DTT reduction. However, this cluster conversion was found to be reversed, yielding primarily the $[4Fe\text{-}4S]^{2+}$ cluster-bound form of homodimeric ^{Nif}IscA, once the capped sample was incubated for 15 min without additional O_2 exposure (broken blue line). Subsequent transient O_2 exposure by removing the cap for 5 min again resulted in reversion to the original $[2Fe\text{-}2S]^{2+}$ cluster-bound form (solid black line) in ~ 65% yield based on initial $[2Fe\text{-}2S]^{2+}$ cluster CD intensity prior to DTT reduction. Although the initial DTT-induced $[2Fe\text{-}2S]^{2+}$ to $[4Fe\text{-}4S]^{2+}$ occurs with breakdown of ~20% of the $[2Fe\text{-}2S]^{2+}$ clusters, as documented by Mössbauer studies, see Table 5, it is remarkable that subsequent cycling between $[4Fe\text{-}4S]^{2+}$ and $[2Fe\text{-}2S]^{2+}$ cluster-bound forms of ^{Nif}IscA occurs with only minor cluster loss as judged by absorption and CD and can be repeated several more times until reduced DTT is fully depleted in the solution. The implication is that the cluster status of ^{Nif}IscA is reversibly responsive to the O_2 levels and the disulfide/dithiol status of the medium. The ability of ^{Nif}IscA to reversibly cycle between $[4Fe\text{-}4S]^{2+}$ and $[2Fe\text{-}2S]^{2+}$ cluster-bound forms in a dithiol redox buffering medium without major cluster degradation in response to cellular O_2 levels is likely to be directly relevant to the role of A-type proteins in the maturation of bacterial [4Fe-4S] cluster-containing proteins under aerobic or oxidative stress growth conditions.

$[4Fe\text{-}4S]^{2+}$ cluster-bound ^{Nif}IscA is competent for in vitro maturation of nitrogenase Fe protein

The ability to obtain forms of ^{Nif}IscA containing exclusively $[2Fe\text{-}2S]^{2+}$ clusters or predominantly [4Fe-4S] clusters afforded the opportunity to investigate if either of these

cluster-bound forms is competent as a cluster donor to apo nitrogenase Fe protein, a potential physiologically relevant [4Fe-4S] cluster-containing acceptor protein. CD spectroscopy involving ADP-bound nitrogenase Fe-protein was used to monitor the time-course of the reaction, since the $[4Fe\text{-}4S]^{2+}$cluster-bound form of ADP-bound nitrogenase Fe-protein has been shown to have an intense and characteristic visible CD spectrum (42), whereas the $[4Fe\text{-}4S]^{2+}$cluster-bound ^{Nif}IscA does not have any significant CD intensity and $[2Fe\text{-}2S]^{2+}$cluster-bound ^{Nif}IscA has an intense and distinctive CD spectrum (see above). The results of cluster transfer using $[4Fe\text{-}4S]^{2+}$ cluster-containing ^{Nif}IscA, generated in situ by treating $[2Fe\text{-}2S]^{2+}$ cluster-containing ^{Nif}IscA with DTT for 15 min, are shown in Figure 8. The ^{Nif}IscA $[4Fe\text{-}4S]^{2+}$ cluster concentration was assessed as approximately 26% of the initial $[2Fe\text{-}2S]^{2+}$ concentration based on parallel Mössbauer studies (see Table 4), and the reaction mixture was designed to have one ^{Nif}IscA $[4Fe\text{-}4S]^{2+}$ cluster (12.5 μM) per dimeric apo nitrogenase Fe protein (12.5 μM). The CD spectrum of apo ADP-bound nitrogenase Fe-protein prior to addition of $[4Fe\text{-}4S]^{2+}$ cluster-containing ^{Nif}IscA (corrected for the final concentration after addition of the ^{Nif}IscA solution) constitutes the zero-time spectrum and CD spectra of the reaction mixture were recorded 4, 8, 15, 25, and 35 min after addition of $[4Fe\text{-}4S]^{2+}$ cluster-containing ^{Nif}IscA. At each time interval, the CD spectra of the residual $[2Fe\text{-}2S]^{2+}$ clusters observed during DTT-induced formation of the $[4Fe\text{-}4S]^{2+}$ clusters on ^{Nif}IscA (see above) have been subtracted from the data shown. The resulting CD spectra are uniquely and quantitatively characteristic of holo ADP-bound nitrogenase Fe-protein (42) and indicate rapid cluster transfer that is 50% complete after 4 min and ~90% complete after 35 min, see Figure 8 (left panel). On the basis of the $[4Fe\text{-}4S]^{2+}$ cluster content of ^{Nif}IscA, the kinetics of $[4Fe\text{-}4S]^{2+}$ cluster transfer as monitored by the CD intensity at 475 nm are well fit with a second order rate constant of 20,000 $M^{-1}min^{-1}$, see Figure 8 (right panel). After 50 min, the individual proteins were separated and repurified using a Q-Sepharose column and quantitative EPR analysis on the dithionite-reduced nitrogenase Fe-protein in the presence of 50% ethylene glycol (to ensure a $S = 1/2$ ground state for the $[4Fe\text{-}4S]^{+}$ clusters (43)) confirmed that at least 90% cluster reconstitution had been achieved (data not shown).

Parallel CD studies in which $[4Fe\text{-}4S]^{2+}$ cluster-bound ^{Nif}IscA was replaced in the cluster transfer mixture with equivalent amounts of S^{2-} and Fe^{2+} compared to cluster concentration did not result in any significant visible CD within 35 min (data not shown). This control experiment demonstrates that the $[4Fe\text{-}4S]^{2+}$ clusters on ^{Nif}IscA are transferred intact to apo ADP-bound nitrogenase Fe-protein, rather than being degraded and then reassembled on apo ADP-bound nitrogenase Fe-protein. In addition, the reaction was repeated under identical conditions with $[2Fe\text{-}2S]^{2+}$ cluster-bound ^{Nif}IscA (25 μM in $[2Fe\text{-}2S]^{2+}$ clusters in final reaction mixture) with no DTT in the reaction mixture. The CD spectra of $[2Fe\text{-}2S]^{2+}$ cluster-bound ^{Nif}IscA was observed and remained unchanged in intensity for at least 40 min indicating that the $[2Fe\text{-}2S]^{2+}$ cluster-bound ^{Nif}IscA is not competent for maturation of apo nitrogenase Fe proteins. Taken together these results clearly demonstrate that only the $[4Fe\text{-}4S]^{2+}$ cluster-bound form of ^{Nif}IscA is competent for maturation of nitrogenase Fe protein under anaerobic conditions and that the maturation process occurs via intact $[4Fe\text{-}4S]^{2+}$ cluster transfer. Moreover, the rate of $[4Fe\text{-}4S]^{2+}$ cluster transfer from ^{Nif}IscA to apo nitrogenase Fe protein is similar to that previously reported for $[4Fe\text{-}4S]^{2+}$ cluster transfer from NifU to apo nitrogenase Fe protein (28), indicating that ^{Nif}IscA offers a viable alternative to NifU for the maturation of [4Fe-4S] cluster containing nitrogen fixation proteins.

In vitro cluster transfer from NifU to apo-^{Nif}IscA

To address the possibility that ^{Nif}IscA serves as a cluster carrier protein that accepts preformed clusters from NifU and delivers them to acceptor proteins, we have investigated

cluster transfer from *A. vinelandii* NifU to ^{Nif}IscA. NifU is a homodimeric modular protein comprising a U-type N-terminal domain, a ferredoxin-type central domain with a redox-active permanent $[2Fe\text{-}2S]^{2+,+}$ cluster, and a Nfu-type C-terminal domain (30;44). Both the N- and C-terminal domains of NifU have been shown to assemble $[4Fe\text{-}4S]^{2+}$ clusters, which can be transferred intact to apo acceptor proteins such as apo-nitrogenase Fe protein (29;30), and NifS-mediated cluster assembly and purification results in a stable form containing one transient $[4Fe\text{-}4S]^{2+}$ cluster and one permanent $[2Fe\text{-}2S]^{2+}$ cluster per NifU monomer (30).

In this study, UV–visible absorption and CD spectroscopy was used to monitor the effect of adding a small excess of apo-^{Nif}IscA to a $[4Fe\text{-}4S]^{2+}$ cluster loaded from of NifU containing one transient $[4Fe\text{-}4S]^{2+}$ cluster and one permanent $[2Fe\text{-}2S]^{2+}$ cluster per NifU monomer under strictly anaerobic conditions, see Figure 9. The reaction mixture was 35 μM in NifU monomer, i.e. 35μM in $[4Fe\text{-}4S]^{2+}$ and permanent $[2Fe\text{-}2S]^{2+}$ clusters, and 100 μM in apo-^{Nif}IscA dimer. The $[4Fe\text{-}4S]^{2+}$ cluster content of the NifU sample was based on Fe and protein determinations and is also evident by the difference in the absorption spectra of as purified NifU containing one permanent $[2Fe\text{-}2S]^{2+}$ cluster (blue line) and the reconstituted and repurified NifU sample used for the cluster transfer studies (red line), see Figure 9. The reaction was carried out in the absence of DTT, but apo-^{Nif}IscA was treated with TCEP and anaerobically repurified prior to use to ensure reduction of disulfides.

Both the absorption and CD data show marked changes on addition of apo-^{Nif}IscA and indicate a rapid reaction that is completed in less than 5 min, as identical spectra were observed for 5, 10, 20, 30 and 50 min after addition of apo-^{Nif}IscA (black lines), see Figure 9, upper and middle panels. The absorption intensity increases and shows better resolved features at ~330, 420, 460 and 550 nm. Both observations are consistent with $[4Fe\text{-}4S]^{2+} \rightarrow 2\times[2Fe\text{-}2S]^{2+}$ cluster conversion, since $\varepsilon_{400} = 15\ mM^{-1}cm^{-1}$ for the $[4Fe\text{-}4S]^{2+}$ cluster on NifU (30) and $\varepsilon_{425} = 10\ mM^{-1}cm^{-1}$ for the $[2Fe\text{-}2S]^{2+}$ cluster on ^{Nif}IscA (see above). Moreover, the resultant absorption spectrum is quantitatively simulated within experimental error as the sum of one permanent $[2Fe\text{-}2S]^{2+}$ cluster on NifU and two $[2Fe\text{-}2S]^{2+}$ clusters on ^{Nif}IscA. Confirmation of this interpretation is provided by the parallel CD spectra. Prior to the addition of ^{Nif}IscA, the CD spectrum of the $[4Fe\text{-}4S]^{2+}$ cluster-loaded NifU (red line) is almost indistinguishable from that of NifU prior to NifS-mediated cluster assembly and replete with permanent $[2Fe\text{-}2S]^{2+}$ clusters (blue line), see Figure 9, indicating that the assembled $[4Fe\text{-}4S]^{2+}$ cluster on NifU has negligible CD intensity. Hence the CD spectrum of the $[2Fe\text{-}2S]^{2+}$ clusters generated by addition of apo-^{Nif}IscA can be assessed by the 50-min minus zero-time difference spectrum. The resulting spectrum is very similar to that of the $[2Fe\text{-}2S]^{2+}$ cluster assembled on ^{Nif}IscA (see Figure 3) and the $\Delta\varepsilon$ values are approximately double those of a single ^{Nif}IscA $[2Fe\text{-}2S]^{2+}$ cluster, indicating that two $[2Fe\text{-}2S]^{2+}$ clusters are formed on ^{Nif}IscA from the single $[4Fe\text{-}4S]^{2+}$ cluster on NifU. The difference CD spectrum is also quite distinct from that of $[2Fe\text{-}2S]^{2+}$ centers on U-type scaffold proteins including the N-terminal domain of NifU (30,44–46), indicating that the clusters are on ^{Nif}IscA rather than NifU. Moreover, anaerobic repurification of ^{Nif}IscA from the reaction mixture, yielded a sample the with characteristic absorption and CD spectra of $[2Fe\text{-}2S]^{2+}$ cluster-bound ^{Nif}IscA.

The observation that cluster transfer involving the $[4Fe\text{-}4S]^{2+}$ cluster assembled on NifU yielded the $[2Fe\text{-}2S]^{2+}$ cluster-bound form of ^{Nif}IscA was not unexpected as the reaction was carried out in the absence of DTT, which appears to be required for stabilizing the $[4Fe\text{-}4S]^{2+}$ cluster-bound form. Nevertheless, it leaves open the question of whether oxidative cleavage of the $[4Fe\text{-}4S]^{2+}$ cluster to yield two $[2Fe\text{-}2S]^{2+}$ cluster occurs on NifU prior to cluster transfer or on ^{Nif}IscA after $[4Fe\text{-}4S]^{2+}$ cluster transfer. We suspect the latter in light of the observation of facile interconversion between $[4Fe\text{-}4S]^{2+}$ and $[2Fe\text{-}2S]^{2+}$

cluster-bound forms of ^{Nif}IscA, with $[2Fe\text{-}2S]^{2+}$-^{Nif}IscA formation being favoured by the absence of DTT and the presence of excess apo-^{Nif}IscA (see below), and control UV–visible absorption and CD experiments that showed no evidence of $[4Fe\text{-}4S]^{2+}$ to $[2Fe\text{-}2S]^{2+}$ cluster conversion on NifU under identical reaction conditions in the absence of ^{Nif}IscA. Attempts to address this question directly via CD-monitored cluster transfer reactions in the presence of 2mM DTT proved to be problematic due to the ability of DTT to partially reduce the permanent $[2Fe\text{-}2S]^{2+}$ cluster on NifU (E_m = −254 mV) (43).

Discussion

A-type proteins are present in the bacterial *isc*, *suf* and *nif* systems as well as the mitochondrial and plastid systems for Fe-S cluster biogenesis, but there is still no consensus concerning their role in the complex process of Fe-S protein maturation. Four different roles have been proposed: alternative scaffolds for assembly of transient Fe-S clusters under aerobic or oxidative stress conditions (17,18,47,48), cluster carriers for the delivery of clusters assembled on primary U-type and SufB-scaffold primary scaffold proteins to apo acceptor proteins (23,35,48), metallochaperones for the delivery of Fe to U-type primary scaffold proteins (16,49–51) or to acceptor proteins to facilitate *in situ* assembly of [4Fe-4S] clusters as indicated in yeast (26). The accompanying manuscript addresses the role of mononuclear Fe-bound forms of ^{Nif}IscA. The results support the view that ^{Nif}IscA can store mononuclear Fe that can be used in Fe-S cluster assembly. However, they do not support a specific role as an immediate iron donor for transient FeS cluster assembly on NifU. Rather a role for Fe-bound in ^{Nif}IscA the in situ assembly or repair of [4Fe-4S] clusters on acceptors is proposed.

The initial observation of cysteine desulfurase-mediated assembly of subunit-bridging [2Fe-2S] and [4Fe-4S] clusters on A-type Fe-S cluster biogenesis proteins (17,47), that can subsequently be transferred to suitable acceptor proteins (47,48,52–54), led to the hypothesis that A-type proteins provide alternative scaffold proteins for assembly of certain types of clusters under specific cellular conditions. This hypothesis is supported by the observation that some recombinant A-type Fe-S cluster biogenesis proteins, including the structurally characterized T. elongatus IscA, contain [2Fe-2S] or [4Fe-4S] clusters as isolated (18,35,55), bacterial gene disruption studies which indicated that IscA/SufA are generally only required for the maturation of [4Fe-4S] cluster-containing proteins under aerobic growth conditions (24), and yeast and human gene disruption studies which implicate an important role for Isa1 and Isa2 in the maturation of mitochondrial [4Fe-4S] clusters (26,36–38,56–58). The alternative scaffold role cannot be completely discounted in bacteria and is supported by the NifS-mediated assembly of $[4Fe\text{-}4S]^{2+}$ clusters on ^{Nif}IscA via $[2Fe\text{-}2S]^{2+}$ cluster intermediates that is presented in this work. Nevertheless, in contrast to U-type primary scaffold proteins (59,60), the lack of evidence for a well-defined cysteine desulfurase/A-type protein complex argues against a role as an alternative primary scaffold for de novo Fe-S cluster biosynthesis.

Moreover, the above observations are also consistent with an alternative hypothesis, namely that that A-type Fe-S cluster biogenesis proteins function as cluster carriers for the delivery of clusters assembled U-type or SufB-type primary scaffold proteins. The cluster carrier hypothesis is supported by *in vitro* studies which indicate that IscA can accept Fe-S clusters from IscU (48) and that SufA can accept Fe-S clusters from the SufBCD complex (61), and recent phylogenomic and genetic studies of the interdependence of the three types A-type Fe-S cluster biogenesis proteins in *E. coli*, i.e. IscA, SufA and ErpA (8,23). IscA and SufA appear to be functionally redundant in *E. coli* (22–24), whereas ErpA is essential for the maturation of the [4Fe-4S] clusters on the IspG and IspH enzymes of the mevalonate-dependent bacterial pathway for the biosynthesis of isopentenyl diphosphate (19). However,

one of the most puzzling aspects of the cluster carrier hypothesis, with respect to the specific role of bacterial A-type proteins in the maturation of [4Fe-4S] cluster-containing proteins under aerobic or oxidative stress conditions, is that cluster transfer from [4Fe-4S] cluster-bound SufBCD results in [2Fe-2S] cluster-bound SufA (61) which itself is competent for the maturation of [4Fe-4S] cluster-containing proteins in the presence of DTT (35).

In this work similar behaviour was observed for ^{Nif}IscA with a $[2Fe\text{-}2S]^{2+}$ cluster-bound form being the product of cluster transfer from [4Fe-4S] cluster-loaded NifU under anaerobic conditions with excess apo-^{Nif}IscA in the absence of DTT. In addition, the [2Fe-2S] cluster-bound ^{Nif}IscA was found to be competent for maturation of the [4Fe-4S] center in the apo nitrogenase Fe protein under anaerobic conditions in the presence of DTT. These results have now been reconciled by the discovery of a reversible equilibrium between forms of ^{Nif}IscA containing one $[2Fe\text{-}2S]^{2+}$ and one $[4Fe\text{-}4S]^{2+}$ cluster per homodimer, with excess DTT being required to generate and stabilize the $[4Fe\text{-}4S]^{2+}$ cluster-bound form under anaerobic conditions and O_2 and/or excess apo-^{Nif}IscA in the absence of DTT resulting in the $[2Fe\text{-}2S]^{2+}$ cluster-bound form.

Based on the available crystallographic data for the [2Fe-2S] cluster-bound form of *T. elongatus* IscA (18), the observation of a $[2Fe\text{-}2S]^{+}$ intermediate in the reductive formation of the $[4Fe\text{-}4S]^{2+}$ cluster-bound form, and the apparent requirement of excess apo-^{Nif}IscA for the oxidative $[4Fe\text{-}4S]^{2+}$ to $[2Fe\text{-}2S]^{2+}$ cluster conversion, a tentative mechanism for this cluster interconversion is presented in Figure 10. The crystal structure suggests an asymmetric dimer structure in solution involving a partially exposed $[2Fe\text{-}2S]^{2+}$ cluster that is asymmetrically coordinated with the conserved cysteines on the α protomer (Cys^{37}, Cys^{101} and Cys^{103}) and the solvent exposed Cys^{103} from the β protomer. DTT is proposed to effect reduction of subunit-bridging $[2Fe\text{-}2S]^{2+}$ cluster to yield a $S = 1/2$ valence-localized $[2Fe\text{-}2S]^{+}$ cluster. This results in weakening of the interaction of the coordinated cysteine of the β protomer leading to dimer dissociation and the transient formation of monomers containing solvent exposed $[2Fe\text{-}2S]^{+}$ clusters that can interact to form valence-delocalized $[4Fe\text{-}4S]^{2+}$ clusters at the interface of a new ^{Nif}IscA dimer. Oxygen or possibly disulfides can then reverse this process via two electron oxidation of the $[4Fe\text{-}4S]^{2+}$ cluster in the presence of apo-^{Nif}IscA, see Fig. 10.

The nature of the physiological electron donor for formation of $[4Fe\text{-}4S]^{2+}$-^{Nif}IscA reductive coupling of $[2Fe\text{-}2S]^{2+}$ clusters has yet to be addressed. However, the inability of cysteine or GSH to promote reductive coupling suggests that it will not occur in the cellular dithiol/disulfide redox buffering medium under aerobic growth conditions (i.e. redox potentials in the range −220 to −270 mV). Consequently the formation of $[4Fe\text{-}4S]^{2+}$-^{Nif}IscA is likely to require anaerobic conditions and a lower potential reductant such as *A. vinelandii* Isc Fdx (E_m = −344 mV) (62). Indeed, in *E. coli* there is direct evidence for a complex between predominantly $[2Fe\text{-}2S]^{2+}$ cluster-bound IscA and Isc Fdx (47). Future experiments are planned to address this hypothesis and the ability of one-electron as well as two-electron donors to induce reductive coupling.

A similar reductive coupling mechanism has been demonstrated for $[4Fe\text{-}4S]^{2+}$ cluster formation on U-type scaffold proteins (11;31;63). Moreover, reductive coupling of two $[2Fe\text{-}2S]^{2+}$ cluster on a U-type scaffold to form a $[4Fe\text{-}4S]^{2+}$ cluster requires similar potentials based on the ability of Isc Fdx to effect partial reduction (64). However there are significant differences. For example, reductive coupling on U-type scaffold proteins requires formation of a form containing two $[2Fe\text{-}2S]^{2+}$ clusters per homodimer and is not reversible as oxygen exposure degrades the subunit-bridging $[4Fe\text{-}4S]^{2+}$ cluster to a more stable form containing one $[2Fe\text{-}2S]^{2+}$ cluster per homodimer (11;63). Hence the ability of A-type proteins to form $[4Fe\text{-}4S]^{2+}$ clusters in a dithiol/disulfide redox buffering medium under

anaerobic conditions and to reversibly interconvert between $[2Fe\text{-}2S]^{2+}$ and $[4Fe\text{-}4S]^{2+}$ cluster-bound forms in response to cellular redox status and/or oxygen levels, provide rationalization for their utility in the maturation of [4Fe-4S] cluster-containing proteins under aerobic growth or oxidative stress conditions. (24).

The implication of the results presented herein for *A. vinelandii* ^{Nif}IscA is that [4Fe-4S] cluster-bound forms are formed, and are competent for maturation of [4Fe-4S] cluster-containing nitrogen fixation apo-proteins via direct cluster transfer, only under anaerobic conditions. *A. vinelandii* is an obligate aerobe that has evolved a number of physiological mechanisms to create an essentially anoxic environment in which nitrogen fixation can occur (64). These include high rates of respiration and the synthesis of a specific protective [2Fe-2S]-Fdx that binds to nitrogenase under oxygen stress conditions to form an inactive enzyme that is protected from damage (64,65). Since NifU is the primary scaffold for [4Fe-4S] cluster assembly (29,30) and is essential for diazotrophic growth (20), whereas ^{Nif}IscA has no observable phenotype (20), it would appear that only NifU is responsible for providing [4Fe-4S] clusters for the maturation of the nitrogenase component proteins NifHDK as well as Fe-S cluster-containing maturation proteins such as the NifEN scaffold and the NifB radical-SAM enzyme. However, in light of the functional redundancy of A-type proteins in *E. coli* and the lack of information on the consequences of a double ^{Nif}IscA/IscA knockout in *A. vinelandii*, this conclusion may be premature. Hence it is still possible that [4Fe-4S] cluster-bound forms of ^{Nif}IscA or IscA may be immediate [4Fe-4S] cluster donors for a subset of nitrogen fixation proteins under anaerobic conditions.

Nevertheless, *in vivo* results in *A. vinelandii* indicate a role for IscA only under oxygen stress conditions (21) and *in vivo* studies in *E. coli* indicate partially redundant roles for the IscA, SufA, and ErpA proteins in the maturation of [4Fe-4S] clusters under aerobic conditions (8,23,24). Under such conditions $[2Fe\text{-}2S]^{2+}$ cluster-bound forms of A-type proteins are likely to be present as a result of cluster transfer from the NifU (this work), IscU (48) or SufB (35) proteins. Hence the question that needs to be addressed is how $[2Fe\text{-}2S]^{2+}$ cluster-bound forms of A-type proteins can be involved in the maturation of [4Fe-4S] cluster containing proteins under aerobic or oxygen stress conditions. Interestingly, a similar role was proposed for the mononuclear Fe-bound form of A-type proteins in the preceding manuscript and is supported by the in vivo evidence that the Fe-bound form the Isa1/Isa2 is required for the maturation of mitochondrial [4Fe-4S] clusters in *S. cerevisiae* under aerobic and anaerobic conditions (26). Based on the resulted presented in the accompanying manuscript, it seems likely that the [2Fe-2S] cluster-bound and Fe(III)-bound forms of A-type proteins may coexist *in vivo* under aerobic conditions in bacteria (25,35). This is further supported by the observation that some Fe(III)-bound ^{Nif}IscA is formed during the O_2-induced [4Fe-4S] to [2Fe-2S] cluster conversion. Hence this raises the possibility that both the Fe-bound and [2Fe-2S] cluster-bound forms of A-type proteins are involved in the maturation of [4Fe-4S] centers on bacterial proteins under aerobic or oxygen stress conditions.

A viable mechanism of how this could occur, based on our recent studies of the mechanism of $[2Fe\text{-}2S]^{2+} \leftrightarrow [4Fe\text{-}4S]^{2+}$ interconversion on the Fumarate Nitrate Reduction (FNR) regulatory protein (66), is presented in detail in the accompanying manuscript. The mechanism is based on the observation that the Fe-S cluster in FNR reversibly cycles between an all-cysteinyl ligated $[4Fe\text{-}4S]^{2+}$ cluster and a $[2Fe\text{-}2S]^{2+}$ cluster with two regular cysteinyl ligands and two cysteine persulfide ligands, with O_2 inducing the $[4Fe\text{-}4S]^{2+}$-to-$[2Fe\text{-}2S]^{2+}$ conversion and Fe(II) and DTT inducing the $[2Fe\text{-}2S]^{2+}$-to$[4Fe\text{-}4S]^{2+}$ conversion. This raises an alternative possibility for in situ $[4Fe\text{-}4S]^{2+}$ cluster assembly on acceptor proteins involving assembly of a cysteine persulfide-ligated $[2Fe\text{-}2S]^{2+}$ cluster on the acceptor protein, via cysteine desulfurase formation of two cysteine persulfides and

delivery of $[2Fe\text{-}2S]^{2+}$ clusters by A-type proteins. Fe-bound A-type proteins would then function in the assembly or repair of O_2-damaged $[4Fe\text{-}4S]^{2+}$ clusters by functioning as the Fe(II) delivery system for transforming the cysteine persulfide-ligated $[2Fe\text{-}2S]^{2+}$ cluster into a conventional $[4Fe\text{-}4S]^{2+}$ center.

Acknowledgments

This work was supported by grants from the National Institutes of Health (GM62542 to M.K.J. and GM47295 to B.H.H.). We thank Dr. Dennis Dean and his coworkers at Virginia Tech for supplying the plasmids for the proteins used in this work.

ABBREVIATIONS

TCEP	tris(2-carboxyethyl)phosphine hydrochloride
DTT	dithiothreitol
FNR	Fumarate Nitrate Reduction regulatory proteins
PLP	pyridoxal phosphate
EPR	Electron Paramagnetic Resonance
GSH	glutathione

References

1. Kiley PJ, Beinert H. The role of Fe-S proteins in sensing and regulation in bacteria. Curr Opin Microbiol. 2003; 6:181–185. [PubMed: 12732309]
2. Fontecave M. Iron-sulfur clusters: ever expanding roles. Nature Chem Biol. 2006; 2:171–174. [PubMed: 16547473]
3. Lill R. Function and biogenesis of iron-sulphur proteins. Nature. 2009; 460:831–838. [PubMed: 19675643]
4. Johnson, MK.; Smith, AD. Encyclopedia of Inorganic Chemistry. 2. King, RB., editor. John Wiley & Sons; Chichester: 2005. p. 2589-2619.
5. Johnson DC, Dean DR, Smith AD, Johnson MK. Structure, function and formation of biological iron-sulfur clusters. Annu Rev Biochem. 2005; 74:247–281. [PubMed: 15952888]
6. Lill R, Mühlenhoff U. Iron-sulfur protein biogenesis in eukaryotes: Components and mechanisms. Annu Rev Cell Dev Biol. 2006; 22:457–486. [PubMed: 16824008]
7. Ayala-Castro C, Saini A, Outten FW. Fe-S cluster assembly pathways in bacteria. Microbiol Mol Biol Rev. 2008; 72:110–125. [PubMed: 18322036]
8. Py B, Barras F. Building Fe-S proteins: bacterial strategies. Nat Rev Microbiol. 2010; 8:436–446. [PubMed: 20467446]
9. Balk J, Pilon M. Ancient and essential: The assembly of iron-sulfur clusters in plants. Trends Plant Sci. 2011; 16:218–226. [PubMed: 21257336]
10. Fontecave M, Ollagnier-de-Choudens S. Iron-sulfur cluster biosynthesis in bacteria: Mechanisms of cluster assembly and transfer. Arch Biochem Biophys. 2008; 474:226–237. [PubMed: 18191630]
11. Bandyopadhyay S, Chandramouli K, Johnson MK. Iron-sulfur cluster biosynthesis. Biochem Soc Trans. 2008; 36:1112–1119. [PubMed: 19021507]
12. Takahashi Y, Nakamura M. Functional assignment of the ORF2-*iscS*-*iscA*-*hscB*-*hscA*-*fdx*-ORF3 gene cluster involved in the assembly of Fe-S clusters in *Escherichia coli*. J Biochem. 1999; 126:917–926. [PubMed: 10544286]
13. Takahashi Y, Tokumoto U. A third bacterial system for the assembly of iron-sulfur clusters with homologs in archaea and plastids. J Biol Chem. 2002; 277:28380–28383. [PubMed: 12089140]

14. Outten FW, Djaman O, Storz G. A *suf* operon requirement for FeS cluster assembly during iron starvation in *Escherichia coli*. Mol Microbiol. 2004; 52:861–872. [PubMed: 15101990]
15. Fontecave M, Ollagnier-de-Choudens S, Py B, Barras F. Mechanisms of iron-sulfur cluster assembly: the SUF machinery. J Biol Inorg Chem. 2005; 10:713–721. [PubMed: 16211402]
16. Ding H, Clark RJ. Characterization of iron-binding in IscA, an ancient iron-sulfur cluster assembly protein. Biochem J. 2004; 379:433–440. [PubMed: 14720122]
17. Krebs C, Agar JN, Smith AD, Frazzon J, Dean DR, Huynh BH, Johnson MK. IscA, an alternative scaffold for Fe-S cluster biosynthesis. Biochemistry. 2001; 40:14069–14080. [PubMed: 11705400]
18. Morimoto K, Yamashita E, Kondou Y, Lee SJ, Arisaka F, Tsukihara T, Nakai M. The asymmetric IscA homodimer with an exposed [2Fe-2S] cluster suggests the structural basis of the Fe-S cluster biosynthetic scaffold. J Mol Biol. 2006; 360:117–132. [PubMed: 16730357]
19. Loiseau L, Gerez C, Bekker M, Ollagnier-de-Choudens S, Py B, Sanakis Y, Teixeira M, Fontecave M, Barras F. ErpA, an iron-sulfur (Fe-S) protein of the A-type essential for respiratory metabolism in *Escherichia coli*. Proc Natl Acad Sci USA. 2007; 104:13626–13631. [PubMed: 17698959]
20. Jacobson MR, Marty R, Cash VL, Weiss MC, Laird NF, Newton WE, Dean DR. Biochemical and genetic analysis of the *nifUSVWZM* from *Azotobacter vinelandii* (1989). Mol Gen Genet. 1989; 219:49–57. [PubMed: 2615765]
21. Johnson DC, Unciuleac M-C, Dean DR. Controlled expression and functional analysis of iron-sulfur cluster biosynthetic components within *Azotobacter vinelandii*. J Bacteriol. 2006; 188:7551–7561. [PubMed: 16936042]
22. Lu J, Yang J, Tan G, Ding H. Complementary roles of SufA and IscA in the biogenesis of iron-sulfur clusters in *Escherichia coli*. Biochem J. 2008; 409:535–543. [PubMed: 17941825]
23. Vinella D, Brochier-Armanet C, Loiseau L, Talla E, Barras F. Iron-sulfur (Fe/S) protein biogenesis: Phylogenomic and genetic studies of A-type carriers. PLoS Genet. 2009; 5:e1000497. [PubMed: 19478995]
24. Tan G, Lu J, Bitoun JP, Huang H, Ding H. IscA/SufA paralogues are required for the [4Fe-4S] cluster assembly in enzymes of multiple physiological pathways in *Escherichia coli* under aerobic growth conditions. Biochem J. 2009; 420:463–472. [PubMed: 19309314]
25. Wang W, Huang H, Tan G, Fan S, Liu M, Landry AP, Ding H. *In vivo* evidence for the iron-binding activity of an iron-sulfur cluster assembly protein IscA in *Escherchia coli*. Biochem J. 2010; 432:429–436. [PubMed: 20942799]
26. Mühlenhoff U, Richter N, Pines O, Pierik AJ, Lill R. Specialized function of yeast Isa1 and Isa2 in the maturation of mitochondrial [4Fe-4S] proteins. J Biol Chem. 2011; 286:41205–41216. [PubMed: 21987576]
27. Drozdzewski PM, Johnson MK. A simple anaerobic cell for low temperature Raman spectroscopy. Appl Spectrosc. 1988; 42:1575–1577.
28. Ravi N, Bollinger JM, Huynh BH, Edmondson DE, Stubbe J. J Am Chem Soc. 1994; 116:8007–8014.
29. Dos Santos PC, Smith AD, Frazzon J, Cash VL, Johnson MK, Dean DR. Iron-sulfur cluster assembly: NifU-directed activation of the nitrogenase Fe-protein. J Biol Chem. 2004; 279:19705–19711. [PubMed: 14993221]
30. Smith AD, Jameson GNL, Dos Santos PC, Agar JN, Naik S, Krebs C, Frazzon J, Dean DR, Huynh BH, Johnson MK. NifS-mediated assembly of [4Fe-4S] clusters in the N- and C-terminal domains of the NifU scaffold protein. Biochemistry. 2005; 44:12955–12969. [PubMed: 16185064]
31. Agar JN, Krebs B, Frazzon J, Huynh BH, Dean DR, Johnson MK. IscU as a scaffold for iron-sulfur cluster biosynthesis: Sequential assembly of [2Fe-2S] and [4Fe-4S] clusters in IscU. Biochemistry. 2000; 39:7856–7862. [PubMed: 10891064]
32. Dailey HA, Finnegan MG, Johnson MK. Human ferrochelatase is an iron-sulfur protein. Biochemistry. 1994; 33:403–407. [PubMed: 8286370]
33. Stephens PJ, Thomson AJ, Dunn JBR, Keiderling TA, Rawlings J, Rao KK, Hall DO. Circular dichroism and magnetic circular dichroism of iron-sulfur proteins. Biochemistry. 1978; 17:4770–4778. [PubMed: 728385]

34. Fu W, Drozdzewski PM, Davies MD, Sligar SG, Johnson MK. Resonance Raman and magnetic circular dichroism studies of reduced [2Fe-2S] proteins. J Biol Chem. 1992; 267:15502–15510. [PubMed: 1639790]
35. Gupta V, Sendra M, Naik SG, Chahal HK, Huynh BH, Outten FW, Fontecave M, Ollagnier de Choudens S. Native *Escherichia coli* SufA, coexpressed with SufBCDSE, purifies as a [2Fe-2S] protein and acts as an Fe-S transporter to Fe-S target enzymes. J Am Chem Soc. 2009; 131:6149–6153. [PubMed: 19366265]
36. Mühlenhoff U, Gerl MJ, Flauger B, Pirner HM, Balser S, Richhardt N, Lill R, Stolz J. The iron-sulfur cluster proteins Isa1 and Isa2 are required for the function but not the de novo synthesis of the Fe/S clusters of biotin synthase in *Saccharomyces cerevisiae*. Eukaryot Cell. 2007; 6:495–504. [PubMed: 17259550]
37. Gelling C, Dawes IW, Richhardt N, Lill R, Muhlenhoff U. Mitochondrial Iba57p is required for Fe/S cluster formation on aconitase and activation of radical SAM enzymes. Mol Cell Biol. 2008; 28:1851–1861. [PubMed: 18086897]
38. Sheftel AD, Wilbrecht C, Stehling O, Niggemeyer B, Elsässer HP, Mühlenhoff U, Lill R. The human mitochondrial ISCA1, ISCA2, and IBA57 proteins are required for [4Fe-4S] protein maturation. Mol Biol Cell. 2012; 23:1157–1166. [PubMed: 22323289]
39. Ferreira GC, Franco R, Lloyd RS, Pereira AS, Moura I, Moura JJG, Huynh BH. Mammalian ferrochelatase, a new addition to the metalloenzyme family. J Biol Chem. 1994; 269:7062–7065. [PubMed: 8125912]
40. Dunham WR, Bearden AJ, Salmeen IT, Palmer G, Sands RH, Orme-Johnson WH, Beinert H. Electronic properties of two-iron, two-sulfur proteins. II Two-iron ferredoxins in spinach, parsley, pig adrenal cortex, *Azotobacter vinelandii* and *Clostridium pasteurianum* Magnetic field Mössbauer spectroscopy. Biochim Biophys Acta. 1971; 253:143–152.
41. Jones DP, Carlsson JL, Mody VC Jr, Cai J, Lynn MJ, Sternberg P Jr. Redox state of glutathione in human plasma. Free Rad Biol Med. 2000; 28:625–635. [PubMed: 10719244]
42. Ryle MJ, Lanzilotta WN, Seefeldt LC, Scarrow RC, Jensen GM. Circular dichroism and X-ray spectroscopies of *Azotobacter vinelandii* nitrogenase iron protein. J Biol Chem. 1996; 271:1551–1557. [PubMed: 8576152]
43. Lindahl PA, Day EP, Kent TA, Orme-Johnson WH, Münck E. Mössbauer, EPR, and magnetization studies of *Azotobacter vinelandii* Fe protein: Evidence for a $[4Fe\text{-}4S]^{1+}$ cluster with spin $S = 3/2$. J Biol Chem. 1985; 260:11160–11173. [PubMed: 2993304]
44. Fu W, Jack RF, Morgan TV, Dean DR, Johnson MK. *nifU* gene product from *Azotobacter vinelandii* is a homodimer that contains two identical [2Fe-2S] clusters. Biochemistry. 1994; 33:13455–13463. [PubMed: 7947754]
45. Yuvaniyama P, Agar JN, Cash VL, Johnson MK, Dean DR. NifS-directed assembly of a transient [2Fe-2S] cluster within the NifU protein. Proc Natl Acad Sci USA. 2000; 97:599–604. [PubMed: 10639125]
46. Chandramouli K, Johnson MK. HscA and HscB stimulate [2Fe-2S] cluster transfer from IscU to apoferredoxin in an ATP-dependent reaction. Biochemistry. 2006; 45:11087–11095. [PubMed: 16964969]
47. Ollagnier-de-Choudens S, Mattioli T, Takahashi Y, Fontecave M. Iron-sulfur cluster assembly. Characterization of IscA and evidence for a specific functional complex with ferredoxin. J Biol Chem. 2001; 276:22604–22607. [PubMed: 11319236]
48. Ollagnier-de-Choudens S, Sanakis Y, Fontecave M. SufA/IscA: reactivity studies of a class of scaffold proteins involved with [Fe-S] cluster assembly. J Biol Inorg Chem. 2004; 9:828–838. [PubMed: 15278785]
49. Ding H, Clark RJ, Ding B. IscA mediates iron delivery for assembly of iron-sulfur clusters in IscU under limited “free” iron conditions. J Biol Chem. 2004; 279:37499–37504. [PubMed: 15247288]
50. Ding B, Smith ES, Ding H. Mobilization of the iron centre in IscA for the iron-sulfur cluster assembly in IscU. Biochem J. 2005; 389:797–802. [PubMed: 15828873]
51. Yang J, Bitoun JP, Ding H. Interplay of IscA and IscU in biogenesis of iron-sulfur clusters. J Biol Chem. 2006; 281:27956–27963. [PubMed: 16877383]

52. Ollagnier-de-Choudens S, Nachin L, Sanakis Y, Loiseau L, Barras F, Fontecave M. SufA from *Erwinia chrysanthemi*Characterization of a scaffold protein required for iron-sulfur cluster assembly. J Biol Chem. 2003; 278:17993–18001. [PubMed: 12637501]
53. Wollenberg M, Berndt C, Bill E, Schwenn JD, Seidler A. A dimer of the FeS cluster biosynthesis protein IscA from cyanobacteria binds a [2Fe2S] cluster between two protomers and transfers it to [2Fe2S] and [4Fe4S] apo proteins. Eur J Biochem. 2003; 270:1662–1671. [PubMed: 12694179]
54. Wu SP, Cowan JA. Iron-sulfur cluster biosynthesis. A comparative kinetic analysis of native and cys-substituted ISA-mediated $[2Fe\text{-}2S]^{2+}$ cluster transfer to an apoferredoxin target. Biochemistry. 2003; 42:5784–5791. [PubMed: 12741836]
55. Zeng J, Geng M, Jiang H, Liu Y, Liu J, Qiu G. The IscA from *Acidithiobacillus ferrooxidans* is an iron-sulfur protein which assemble the $[Fe_4S_4]$ cluster with intracellular iron and sulfur. Arch Biochem Biophys. 2007; 463:237–244. [PubMed: 17470358]
56. Jensen LT, Culotta VC. Role of *Saccharomyces cerevisiae* Isa1 and Isa2 in iron homeostasis. Mol Cell Biol. 2000; 20:3918–3927. [PubMed: 10805735]
57. Kaut A, Lange H, Diekert K, Kispal G, Lill R. Isa1p is a component of the mitochondrial machinery for maturation of cellular iron-sulfur proteins and requires conserved cysteine residues for function. J Biol Chem. 2000; 275:15955–15961. [PubMed: 10748136]
58. Pelzer W, Mühlenhoff U, Diekert K, Siegmund K, Kispal G, Lill R. Mitochondrial Isa2p plays a crucial role in the maturation of cellular iron-sulfur proteins. FEBS Lett. 2000; 476:134–139. [PubMed: 10913600]
59. Shi R, Proteau A, Villarroya M, Moukadiri I, Zhang L, Trempe J-F, Matte A, Armengod ME, Cygler M. Structural basis for Fe-S cluster assembly and tRNA thiolation mediated by IscS protein-protein interactions. PLoS Biology. 2010; 8:e1000354. [PubMed: 20404999]
60. Marinoni EN, de Oliveira JS, Nicolet Y, Raulfs EC, Amara P, Dean DR, Fontecilla-Camps JC. $(IscS\text{-}IscU)_2$ complex structures provide insights into Fe_2S_2 biogenesis and transfer. Angew Chem Int Ed. 2012; 51:5439–5442.
61. Chahal HK, Dai Y, Saini A, Ayala-Castro C, Outten FW. The SufBCD Fe-S scaffold complex interacts with SufA for Fe-S cluster transfer. Biochemistry. 2009; 48:10644–10653. [PubMed: 19810706]
62. Jung YS, Gao-Sheridan HS, Christiansen J, Dean DR, Burgess BK. Purification and biophysical characterization of a new [2Fe-2S] ferredoxin from *Azotobacter vinelandii*, a putative [Fe-S] cluster assembly/repair protein. J Biol Chem. 1999; 274:32402–32410. [PubMed: 10542283]
63. Chandramouli K, Unciuleac M-C, Naik S, Dean DR, Huynh BH, Johnson MK. Formation and properties of [4Fe-4S] clusters on the IscU scaffold protein. Biochemistry. 2007; 46:6804–6811. [PubMed: 17506525]
64. Setubal JC, et al. Genome sequence of *Azotobacter vinelandii,* an obligate aerobe specialized to support diverse anaerobic metalbolic processes. J Bacteriol. 2009; 191:4534–4545. [PubMed: 19429624]
65. Moshiri F, Kim JW, Maier RJ. The FeSII protein of *Azotobacter vinelandii* is not essential for aerobic nitrogen fixation, but confers significant protection to oxygen-mediated inactivation of nitrogenase in vitro and in vivo. Mol Microbiol. 1994; 14:101–114. [PubMed: 7830548]
66. Zhang B, Crack JC, Subramanian S, Green J, Thomson AJ, Le Brun NE, Johnson MK. Reversible cycling between cysteine persulfide-ligated [2Fe-2S] and cysteine-ligated [4Fe-4S] clusters in the FNR regulatory protein. Proc Natl Acad Sci USA. 2012 in press.

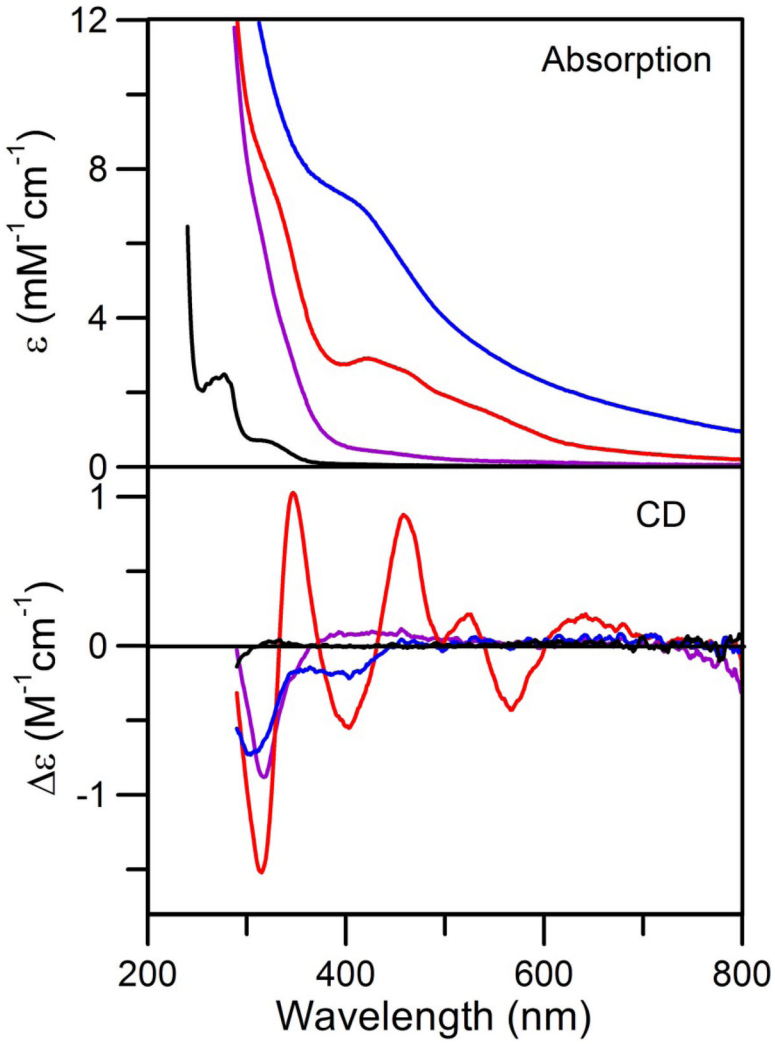

Figure 1.

NifS-mediated Fe-S cluster assembly on ^{Nif}IscA monitored as a function of time by UV–visible absorption and CD spectroscopy. Protein and reagent concentrations are described in the Experimental Procedures. The spectra shown are for TCEP pre-treated apo-^{Nif}IscA before reconstitution (black) and after 5 min (purple), 20 min (red), and 65 min (blue) of NifS-mediated Fe-S cluster assembly. ε and Δε values are expressed per ^{Nif}IscA monomer.

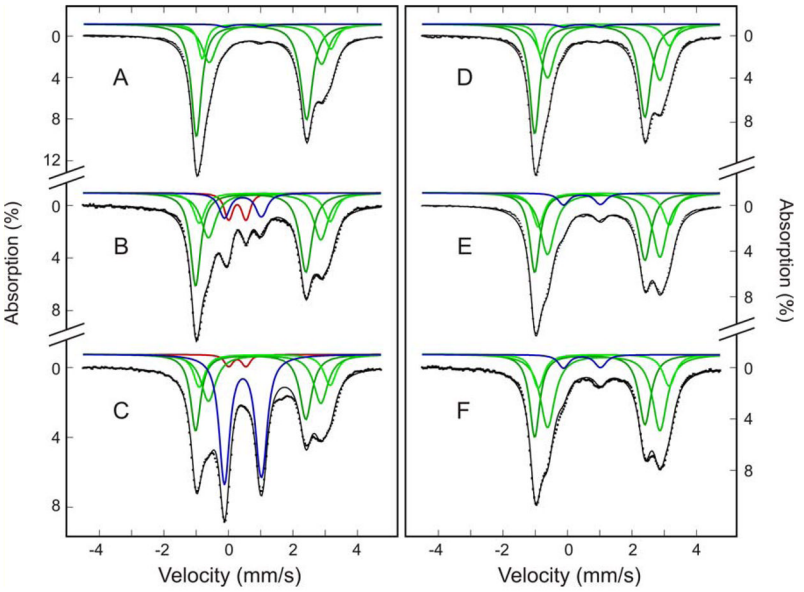

Figure 2.

Time-dependent Mössbauer spectra of NifS-mediated Fe-S cluster assembly on ^{Nif}IscA. The reconstitution mixture with (left panel) and without (right panel) ^{Nif}IscA was frozen at time intervals of 2 min (A and D), 20 min (B and E), and 60 min (C and F). See Experimental Procedures for protein and reagent concentrations. The Mössbauer spectra (dotted lines) were recorded at 4.2 K in a magnetic field of 50 mT applied parallel to the γ-beam. The colored lines are theoretical simulations for the individual Fe species using the parameters listed in Table 1: $Fe^{II}Cys_4$, Fe^{II}-3.5 and Fe^{II}-4.1 in green; $[2Fe\text{-}2S]^{2+}$ cluster in red; $[4Fe\text{-}4S]^{2+}$ cluster in blue. They are plotted in accord with the percentage absorptions listed in Table 2. The solid black lines overlaid with the experimental spectra are composites of the simulations shown.

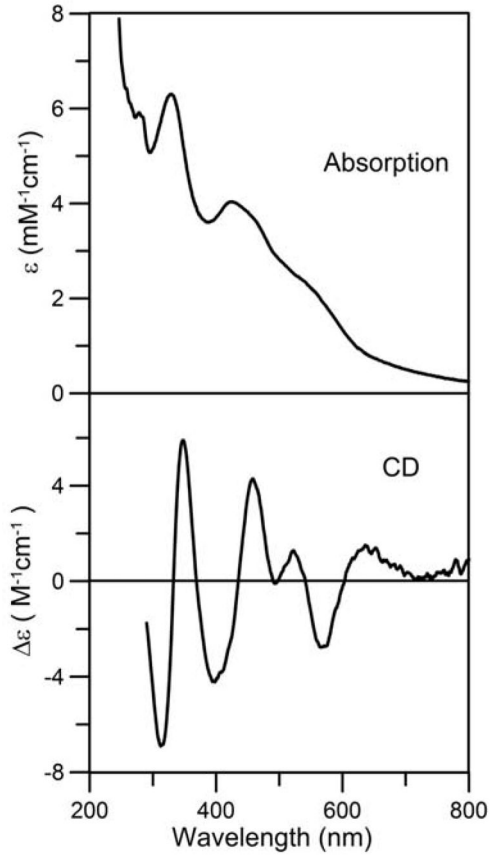

Figure 3.

UV–visible absorption and visible CD spectra of the purified $[2Fe\text{-}2S]^{2+}$ cluster-bound form of ^{Nif}IscA recorded at room temperature under anaerobic conditions in septum-sealed 1 mm quartz cuvettes. Molar extinction coefficients (ε) values are based on the concentration of monomeric ^{Nif}IscA as determined by protein assays and Δε values are based on the concentration of ^{Nif}IscA-bound $[2Fe\text{-}2S]^{2+}$ clusters.

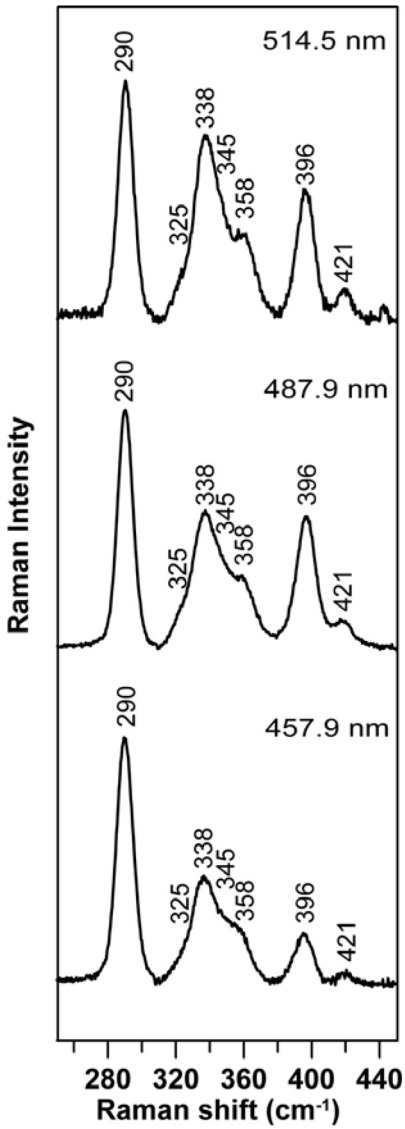

Figure 4.

Resonance Raman spectra of purified -bound form of ^{Nif}IscA. Raman spectra were recorded at 17 K with 457.9, 487.9 and 514.5 nm laser excitation with ~ 185 mW laser power at the sample. The sample (~2 mM in $[2Fe\text{-}2S]^{2+}$ clusters) was in 100 mM Tris-HCl buffer, pH 7.8 containing ~ 0.45 M NaCl. Each spectrum is a sum of 100 scans, with each scan involving counting photons for 1 s at 0.5 cm^{-1} increments with 6 cm^{-1} spectral resolution. Bands due to lattice modes of ice from frozen buffer in sample have been subtracted from all spectra.

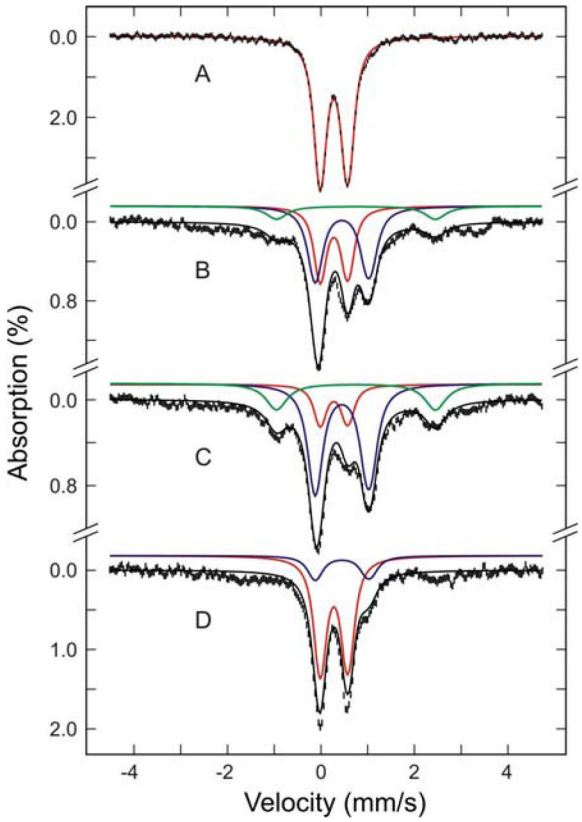

Figure 5.

DTT-induced $[2Fe\text{-}2S]^{2+}$-to-$[4Fe\text{-}4S]^{2+}$ cluster conversion and O_2-induced $[4Fe\text{-}4S]^{2+}$-to-$[2Fe\text{-}2S]^{2+}$ cluster conversion on ^{Nif}IscA monitored by Mössbauer spectroscopy. Mössbauer spectra (hashed marks) were recorded at 4.2 K in a magnetic field of 50 mT applied parallel to the γ-beam. The spectra shown are for reconstituted and repurified $[2Fe\text{-}2S]^{2+}$ cluster-bound ^{Nif}IscA (0.5 mM in $[2Fe\text{-}2S]^{2+}$ clusters) prior to addition of 2.0 mM DTT (A), 1 min after DTT addition (B), 15 min after DTT addition (C), and after exposing the 15 min DTT-treated sample to air for 5 min (D). The colored lines are theoretical simulations for the individual Fe species (Fe(II) species in green, $[2Fe\text{-}2S]^{2+}$ clusters in red and $[4Fe\text{-}4S]^{2+}$ clusters in blue) using the parameters listed in Table 4 and plotted in percentages listed in Table 5. The solid black lines overlaid with the experimental spectra are the composite spectra.

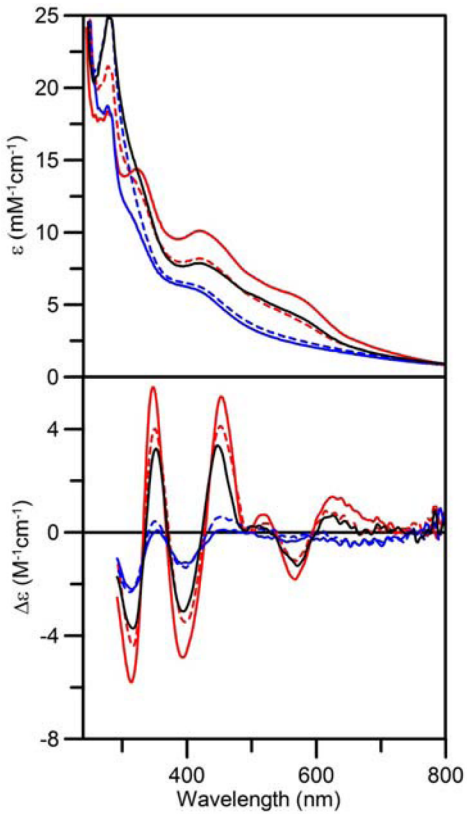

Figure 6.

$[2Fe\text{-}2S]^{2+} \leftrightarrow [4Fe\text{-}4S]^{2+}$ cluster interconversions on ^{Nif}IscA monitored by UV–visible absorption and CD spectroscopies. Anaerobically purified $[2Fe\text{-}2S]^{2+}$ cluster-bound (solid red line) was treated with 2 mM DTT and incubated for 15 min (solid blue line), exposed to air for 5 min (broken red line), sealed and incubated for an additional 15 min (broken blue line), and exposed to air again for 5 min (solid black line). ε and Δε values are based on the $[2Fe\text{-}2S]^{2+}$ cluster concentration of the initial $[2Fe\text{-}2S]^{2+}$ cluster-bound ^{Nif}IscA sample (0.05 mM). The CD spectra of the first and second air-exposed samples have been corrected for contributions from Fe(III)-bound ^{Nif}IscA, by subtracting CD spectra of Fe(III)-bound ^{Nif}IscA (see accompanying manuscript) corresponding to 10% and 20% of the total Fe, respectively.

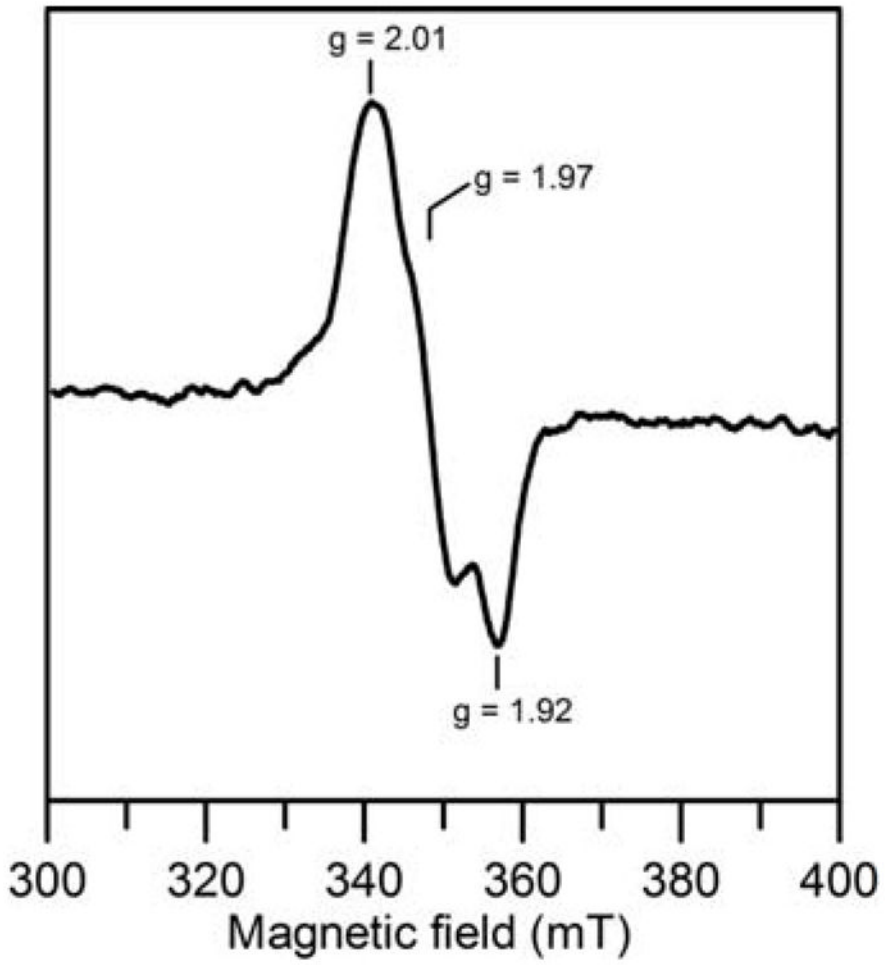

Figure 7.

X-band EPR spectrum of $[2Fe\text{-}2S]^{2+}$ cluster-bound ^{Nif}IscA after addition of DTT. Sample was frozen within 5 s of the addition of 2 mM DTT and the spectrum was recorded at 30 K using 10 mW microwave power, using a modulation amplitude of 0.63 mT and a microwave frequency of 9.60 GHz.

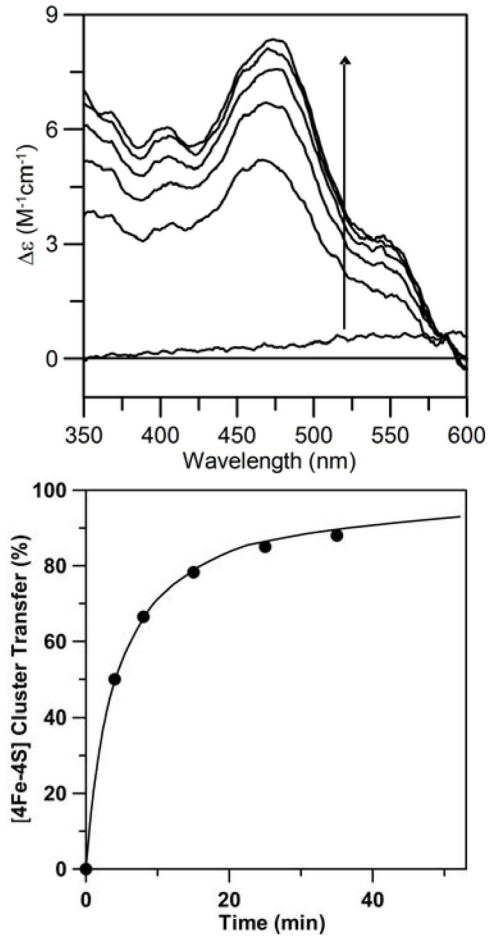

Figure 8.

Time course of cluster transfer from $[4Fe\text{-}4S]^{2+}$ cluster-bound ^{Nif}IscA to *A. vinelandii* apo ADP-bound nitrogenase Fe protein monitored by UV–visible CD spectroscopy under anaerobic conditions. Right panel: CD spectra of apo ADP-bound nitrogenase Fe protein (12.5 μM in dimer in final reaction mixture) were recorded before (zero time) and after reaction with $[4Fe\text{-}4S]^{2+}$ cluster-bound ^{Nif}IscA (12.5 μM in $[4Fe\text{-}4S]^{2+}$ clusters in the final reaction mixture) for 4, 8, 15, 25, and 35 min. The arrow indicates an increase in CD intensity with increasing time. Δε values are based on the initial ^{Nif}IscA $[4Fe\text{-}4S]^{2+}$ cluster concentration. Left panel: Kinetics of $[4Fe\text{-}4S]^{2+}$ cluster based on CD intensity of holo ADP-bound nitrogenase Fe protein at 475 nm as function of time. The solid line is the best fit kinetic simulation for direct cluster transfer with a second order rate constant of 20,000 $M^{-1}min^{-1}$.

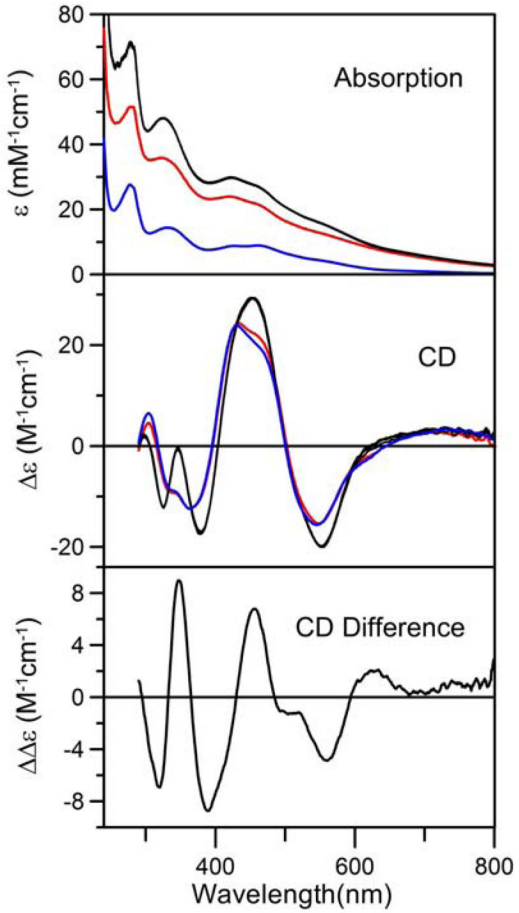

Figure 9.

Time course of cluster transfer from $[4Fe\text{-}4S]^{2+}$ cluster-bound NifU to apo- ^{Nif}IscA monitored by UV–visible absorption and CD spectroscopy under anaerobic conditions at room temperature in the absence of DTT. Upper and middle panels show UV–visible absorption and CD spectra of the reaction mixture containing $[4Fe\text{-}4S]^{2+}$ cluster-bound NifU (35 μM in NifU monomer with one $[4Fe\text{-}4S]^{2+}$ clusters and one permanent $[2Fe\text{-}2S]^{2+}$ cluster per monomer) and apo-^{Nif}IscA (100 μM in ^{Nif}IscA dimer) recorded before addition of apo-^{Nif}IscA (zero time, red lines) and 5, 10, 20, 30, and 50 min after addition of apo-^{Nif}IscA (overlapping black lines). The UV–visible absorption and CD spectra of NifU containing only the permanent $[2Fe\text{-}2S]^{2+}$ cluster are shown for comparison (blue lines). The lower panel shows the 50 min minus zero time difference CD spectrum that is characteristic of $[2Fe\text{-}2S]^{2+}$ cluster-bound ^{Nif}IscA. All ε, Δε, and ΔεΕ values are expressed per NifU monomer.

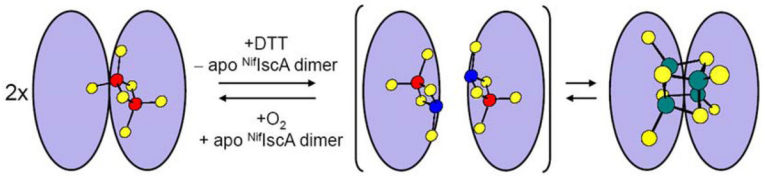

Figure 10.
Proposed mechanism for $[2Fe\text{-}2S]^{2+}$ and $[4Fe\text{-}4S]^{2+}$ cluster interconversion on ^{Nif}IscA (red, Fe^{3+}; blue Fe^{2+}; green, $Fe^{2.5+}$; yellow, S).

Table 1

Mössbauer parameters of the Fe species detected during Fe–S cluster assembly and $[4Fe\text{-}4S]^{2+}$ and $[2Fe\text{-}2S]^{2+}$ cluster interconversions on ^{Nif}IscA

Fe species	δ (mm/s)[a]	ΔE_Q (mm/s)[a]
Fe^{II}-4.1	1.16	4.06
Fe^{II}-3.5	1.12	3.48
Fe^{II}Cys4	0.69	3.42
Fe(II)	0.75	3.40
$[2Fe\text{-}2S]^{2+}$		
Site 1	0.27	0.50
Site 2	0.28	0.68
$[4Fe\text{-}4S]^{2+}$		
Pair 1	0.46	1.25
Pair 2	0.44	1.04

[a]The estimated uncertainties for δ and ΔE_Q are 0.02 and 0.04 mm/s, respectively.

Table 2

Analysis of Mössbauer resonances as a percentage of total Fe during NifS-mediated Fe-S cluster assembly on ^{Nif}IscA as a function of reaction time. Values in parentheses are estimated uncertainties for the last significant digits.

Sample	reaction time (min)	$Fe^{II}Cys_4$	Fe^{II}-3.5	Fe^{II}-4.1	$[2Fe\text{-}2S]^{2+}$	$[4Fe\text{-}4S]^{2+}$
^{Nif}IscA (−) (control)	2	51 (5)	36 (4)	11 (2)	–	2 (2)
^{Nif}IscA (+)	2	56 (5)	28 (3)	14 (2)	–	2 (2)
^{Nif}IscA (−) (control)	20	36 (4)	41 (4)	18 (2)	–	5 (2)
^{Nif}IscA (+)	20	39 (4)	27 (3)	14 (2)	9 (2)	11 (2)
^{Nif}IscA (−) (control)	60	34 (4)	44 (5)	16 (2)	–	6 (2)
^{Nif}IscA (+)	60	24 (3)	21 (3)	11 (2)	3 (2)	41 (4)

Table 3

Fe–S stretching frequencies (cm^{-1}) and assignments for the $[2Fe\text{-}2S]^{2+}$ centers in *A. vinelandii* ^{Nif}IscA, *S. oleracea* ferredoxin, bovine adrenodoxin, and *P. putida* putidaredoxin.

Mode (D_{2h})[a]	Ferredoxin[b]	Adrenodoxin[b]	Putidaredoxin[b]	*A. vinelandii* ^{Nif}IscA
$B2u^b$	427	421	426	421
Ag^b	395	393	400	396
$B3u^b$	367	349	350	358
$B1u^t$, $B2g^t$	357	341	344	~345
Ag^t	338	329	338	338
$B1g^b$	329	317	320	~325
$B3u^t$	283	291	291	290

[a] Symmetry labels under idealized D_{2h} symmetry for a $Fe_2S_2bS_4t$ unit, where S^b and S^t indicate bridging and terminal (cysteinyl) S, respectively.

[b] Taken from reference 34

Table 4

Analysis of Mössbauer resonances as a percentage of total Fe during $[2Fe\text{-}2S]^{2+}/[4Fe\text{-}4S]^{2+}$ cluster conversions on ^{Nif}IscA. Values in parentheses are estimated uncertainties for the last significant digits.

Sample	$[2Fe\text{-}2S]^{2+}$	$[4Fe\text{-}4S]^{2+}$	Fe^{II}	remaining Fe[a]
Reconstituted $[2Fe\text{-}2S]^{2+}$ ^{Nif}IscA (Sample A)	100	–	–	–
Sample A treated with 2 mM DTT for 1 min	34 (4)	43 (4)	10 (2)	13 (2)
Sample A treated with 2 mM DTT for 15 min	16 (3)	53 (5)	18 (3)	13 (2)
Sample A treated with 2 mM DTT for 15 min and air for 5 min	60 (5)	15 (3)	–	25 (3)

[a]The remaining Fe is primarily in the form a $S = 1/2$ $[2Fe\text{-}2S]^{+}$ cluster for the samples treated with DTT for 1 min and 15 min and in the form of $S = 3/2$ Fe(III)-bound ^{Nif}IscA for the sample treated with DTT and then exposed to air (see text for details).